UTTG-04-96
hep-th/9603170
25 March 1996, revised 6 May 1996, 19 March 1997

Duality Between the Webs of Heterotic and Type II Vacua

Philip Candelas[1] and Anamaría Font[2]

Theory Group
Department of Physics
University of Texas
Austin, TX 78712, USA

ABSTRACT

We discuss how transitions in the space of heterotic $K3 \times T^2$ compactifications are mapped by duality into transitions in the space of Type II compactifications on Calabi–Yau manifolds. We observe that perturbative symmetry restoration, as well as non-perturbative processes such as changes in the number of tensor multiplets, have at least in many cases a simple description in terms of the reflexive polyhedra of the Calabi–Yau manifolds. Our results suggest that to many, perhaps all, four-dimensional $N = 2$ heterotic vacua there are corresponding type II vacua.

[1] candelas@physics.utexas.edu.

[2] afont@dino.conicit.ve. On sabbatical leave from Departamento de Física, Facultad de Ciencias, Universidad Central de Venezuela.

Contents

1. **Introduction**

In this paper we explore four-dimensional, $N = 2$ string vacua in connection with the conjectured duality [1,2] between $(0, 4)$ compactifications of the $E_8 \times E_8$ heterotic string on the manifold $K3 \times T^2$ and the type IIA string compactified on a Calabi-Yau manifold. This duality has been the subject of several articles in the recent literature [3-11]. Schematically we may write

$$\mathrm{Het}_{E_8\times E_8}\big[K3 \times T^2,\, \mathcal{V}\big] \simeq \mathrm{IIA}\big[\mathcal{M}\big]$$

where $\mathcal{V}$ denotes the bundle (more properly a sheaf) corresponding to the background gauge field and $\mathcal{M} = \mathcal{M}_{\mathcal{V}}$ a Calabi–Yau manifold that depends on $\mathcal{V}$. This duality induces a correspondence

$$\mathcal{V} \leftrightarrow \mathcal{M}_{\mathcal{V}}$$

between vector bundles on $K3\times T^2$ and certain (perhaps all) Calabi–Yau manifolds, though a special role is played by manifolds that are $K3$-fibrations [3,4,9]. The evidence supporting this correspondence is based on the identification of certain dual pairs $(\mathcal{V}, \mathcal{M}_{\mathcal{V}})$ through a computation of Hodge numbers and, very compellingly, on detailed comparison of the structure of the moduli-spaces of $\mathcal{V}$ and $\mathcal{M}_{\mathcal{V}}$ for candidate dual pairs previously identified on the basis of their Hodge numbers[1,6,7,12,13].

Two observations concerning this duality are the subject of the present article: that a great many Calabi–Yau manifolds are known in terms of toric data[14-17] and the correspondence, pointed out by Batyrev, between Calabi–Yau manifolds and reflexive polyhedra [18]. Proceeding loosely: we have a correspondence between reflexive polyhedra, Δ, and Calabi–Yau manifolds $\mathcal{M}_\Delta$. Combining this with the correspondence between vector bundles $\mathcal{V}$ and Calabi–Yau manifolds gives a correspondence between vector bundles on $K3 \times T^2$ and reflexive polyhedra $\mathcal{V} = \mathcal{V}_\Delta$. It is known also that the moduli spaces of Calabi–Yau manifolds form a web in which continuous transitions between different Calabi–Yau manifolds (phases) occur due to the shrinking to zero of certain homology two cycles and three cycles as the parameters of the manifold are varied[19-22]. Indeed it seems likely that all Calabi–Yau manifolds are connected by processes of this type[23-26]. The consistency and continuity of the string vacua associated with this process is assured by effects involving solitons that wrap the vanishing cycles and which become massless at the transition where the cycles vanish[27-30]. In virtue of duality this web structure must exist also on the heterotic side, though the physical picture is different. Indeed, the space

of heterotic vacua also forms a web in which different models are connected along branches parametrized by vacuum expectation values of scalars in vector and hypermultiplets that correspond to the parameters of $\mathcal{V}$. In virtue of the correspondence $\mathcal{V} \leftrightarrow \Delta$ there should be a dictionary that translates between the language of reflexive polyhedra and that of heterotic dynamics, including the non-perturbative effects uncovered by new insight into string phenomena [31-33]. A first step towards finding such dictionary was taken in ref. [8] where it was noticed that un-Higgsing of $SU(r)$ groups in certain heterotic models matched with a chain of $K3$ fibrations. Subsequently, it was argued that the appearance of perturbative heterotic groups in these chains could be explained in the Calabi-Yau picture as well [10].

Motivated by the observations of [8], we point out that corresponding to a Higgsing chain of heterotic models, there is a chain of Calabi–Yau manifolds with a simple structure revealed by their description in terms of reflexive polyhedra. These manifolds are $K3$ fibrations. Indeed the four-dimensional polyhedron contains the polyhedron of the $K3$ in a simple way and it is this nesting of polyhedra that motivates much of our analysis. One notable point is that the Dynkin diagram of the group and also the extended Dynkin diagram can be seen in the edges of the $K3$ polyhedron.

The heterotic models of [8] basically correspond to $K3 \times T^2$ compactifications in which instanton numbers $(d_1, d_2) = (24, 0), (20, 4), (18, 6), (16, 8)$ and $(14, 10)$ are embedded in $E_8 \times E_8$ [34]. Maximally Higgsing the initial gauge group leads to models that can be identified with type II compactifications on known $K3$ fibrations [1,8,35]. Starting at these 'irreducible models', we then study the type II description of symmetry restoration of different group factors. Recent results of ref. [35] allow us to consider other values of (d_1, d_2). In some cases we find it necessary to include the effect of $D = 6$ extra tensor multiplets in the heterotic construction [33]. Reversing our strategy, we have also analyzed type II processes that arguably correspond to non-perturbative heterotic effects. The resulting type II pattern strongly suggests that these processes indeed have a non-perturbative interpretation in terms of transitions in which the number of tensor multiplets jumps by one and an instanton shrinks to zero.

This note is organized as follows. In section 2 we analyze $K3$ and $K3 \times T^2$ heterotic compactifications, including possible symmetry breaking patterns. Theories of this kind have been studied in recent related work [32,33,35-38]. In section 3 we consider various sequences of reflexive polyhedra and determine their relation to heterotic models. In section 4 we present our conclusions and list some open questions. An appendix contains tables of Hodge numbers and figures of the polyhedra that we discuss.

2. **Heterotic Chains**

The starting point is a heterotic $E_8 \times E_8$ compactification on $K3$ with $SU(2)$ bundles with instanton numbers (d_1, d_2) such that $d_1 + d_2 = 24$. When both $d_i \geq 4$, the resulting group is the commutant of the instantons which is $E_7 \times E_7$ with massless hypermultiplets transforming as **56**s and/or singlets under each E_7. Using the index theorem we find the hypermultiplet spectrum

$$\frac{1}{2}(d_1 - 4)(\mathbf{56}, \mathbf{1}) + \frac{1}{2}(d_2 - 4)(\mathbf{1}, \mathbf{56}) + 62(\mathbf{1}, \mathbf{1}) \ .$$

When $d_1 = 24$, $d_2 = 0$, the gauge group is $E_7 \times E_8$ and the massless hypermultiplets include

$$10(\mathbf{56}, \mathbf{1}) + 65(\mathbf{1}, \mathbf{1}) \ .$$

Without loss of generality we can take $12 \leq d_1 \leq 20$, unless $d_1 = 24$. We also find it convenient to define

$$k \stackrel{\text{def}}{=} \frac{d_1 - 12}{2} \ . \tag{2.1}$$

Since the **56** of E_7 is a pseudoreal representation, the d_i can be odd and k can be half-integer.

An initial heterotic model can be deformed by vevs of hypermultiplets thereby breaking the gauge group. Since $d_1 \geq 12$, the number of $(\mathbf{56}, \mathbf{1})$'s is such that the first E_7 can be completely broken. In particular, it can be broken through the chain

$$E_7 \to E_6 \to SO(10) \to SU(5) \to SU(4) \to SU(3) \to SU(2) \to SU(1) \ , \tag{2.2}$$

where $SU(1)$ denotes the trivial group consisting of the identity only. On the other hand, the group arising from the second E_8 can only be broken to some terminal group $G_2^{(0)}$ that depends on k. For instance, $G_2^{(0)}(k) = E_8, E_7, E_6, SO(8)$ for $k = 6, 4, 3, 2$ and $G_2^{(0)}(k) = SU(1)$ for $k = 1, 0$.

The hypermultiplet content at every stage of breaking can of course be derived by group theory but it can also be found by imposing anomaly factorization conditions. Recall that the anomaly eight-form is given by

$$I_8 = \frac{1}{16(2\pi)^4}(\mathrm{tr}R^2 - v_\alpha \mathrm{tr}F_\alpha^2)(\mathrm{tr}R^2 - \tilde{v}_\alpha \mathrm{tr}F_\alpha^2) \ ,$$

where α runs over the various gauge factors. At Kac-Moody level one, the coefficients v_α are given by $v_\alpha = 2, 1, \frac{1}{3}, \frac{1}{6}, \frac{1}{30}$ for $\alpha = SU(N), SO(2N), E_6, E_7, E_8$ respectively [39]. The coefficients $\tilde{v}_\alpha$ depend on the hypermultiplet spectrum and can be determined from the form of the total anomaly [39]. For instance,

$$\begin{aligned} &\tilde{v}_{E_8} = -\frac{1}{5}, \qquad \tilde{v}_{E_7} = \frac{n_{56}-4}{6}, \qquad \tilde{v}_{E_6} = \frac{n_{27}-6}{6}, \quad \tilde{v}_{SO(10)} = \frac{n_{16}-4}{2}, \\ &\tilde{v}_{SU(5)} = n_{10} - 2, \quad \tilde{v}_{SU(4)} = n_6 - 2, \quad \tilde{v}_{SU(3)} = \frac{n_3-18}{6}, \quad \tilde{v}_{SU(2)} = \frac{n_2-16}{6}, \end{aligned} \tag{2.3}$$

where n_R is the number of hypermultiplets in the R representation. In the case of $SO(10)$, $SU(5)$, and $SU(4)$, the number of fundamental representations is constrained to be $n_{10} = 2 + n_{16}$, $n_5 = 10 + 3n_{10}$ and $n_4 = 8 + 4n_6$ respectively. Finally, the total number of vector multiplets, n_V and hypermultiplets, n_H, satisfy the condition

$$n_H - n_V = 244 \ . \tag{2.4}$$

It is easy to check that (2.4) is satisfied in the initial (d_1, d_2) models described above.

In general, the gauge group is of the form $G = G_1 \times G_2$, with G_1 and G_2 coming from the first and second E_8's. These groups are themselves products of simple factors. Notice that before Higgsing we have

$$\frac{\tilde{v}_1}{v_1} = k \qquad , \qquad \frac{\tilde{v}_2}{v_2} = -k \ , \tag{2.5}$$

where we have assumed $d_1 + d_2 = 24$ (more generally $\tilde{v}_2/v_2 = (d_2 - 12)/2$). After Higgsing, all non-Abelian factors contained in G_2 will satisfy $\tilde{v}_\alpha/v_\alpha = -k$. In particular, this implies that the terminal groups $G_2^{(0)}(k)$ mentioned above are free of charged matter. Similarly, all non-Abelian factors contained in G_1 will satisfy $\tilde{v}_\alpha/v_\alpha = k$. For instance, if the first E_7 is broken to $SU(2)$, the number of doublets turns out to be

$$n_2 = 12k + 16 \ . \tag{2.6}$$

The number of $SU(2)$ singlets is obtained from (2.4). For example, if G is broken to $SU(2) \times G_2^{(0)}(k)$, we find

$$n_1 = 215 + \dim G_2^{(0)}(k) - 24k \ . \tag{2.7}$$

It is straightforward to repeat this sort of analysis for other breaking patterns.

Up to now we have focused on six-dimensional models. Upon further compactification on T^2, the $N=1$, $d=6$ hyper and vector multiplets of G give rise to $N=2$, $d=4$ hyper and vector multiplets also of G, in numbers n_H and n_V that still must fulfill (2.4). The tensor multiplet produces an extra $U(1)$ vector multiplet associated to the dilaton and for generic 2-torus shape, there also appear two extra $U(1)$ vector multiplets corresponding to the torus that are usually denoted by T and U. Another new feature is the existence of a Coulomb branch parametrized by expectation values of the adjoint scalars in the $N=2$ vector multiplets. At a generic point, excluding the graviphoton, the gauge group is $U(1)^{\operatorname{rank} G+3}$ and the massless hypermultiplets include those n^G_{sing} fields originally neutral under G.

An $N=2$, $D=4$ heterotic model with the structure just described is potentially equivalent to a type IIA compactification on a Calabi–Yau manifold that is a $K3$ fibration and has

$$\begin{aligned} h_{11} &= \operatorname{rank} G + 3 \\ h_{12} &= n^G_{sing} - 1 \ . \end{aligned} \tag{2.8}$$

In particular, maximal Higgsing of G to the matter-free $G_2^{(0)}(k)$ leads to

$$\begin{aligned} h_{11} &= \operatorname{rank} G_2^{(0)}(k) + 3 \\ h_{12} &= 243 + \dim G_2^{(0)}(k) \ . \end{aligned} \tag{2.9}$$

Un-Higgsing an $SU(2)$ factor in G_1 then changes these numbers to

$$\begin{aligned} h_{11} &= \operatorname{rank} G_2^{(0)}(k) + 4 \\ h_{12} &= 214 + \dim G_2^{(0)}(k) - 24k \ . \end{aligned} \tag{2.10}$$

Another interesting situation is the un-Higgsing of $SU(2)\times SU(2)$. In this case we find

$$\begin{aligned} h_{11} &= \operatorname{rank} G_2^{(0)}(k) + 5 \\ h_{12} &= 185 + \dim G_2^{(0)}(k) - 40k \ . \end{aligned} \tag{2.11}$$

Similar results can be derived for other symmetry restoration patterns.

For $k=6,4,3,2,1$, eqs. (2.9) yield Hodge numbers that match those of known $K3$ fibrations given by hypersurfaces of degree $12k+12$ in $\mathbb{P}_4(1,1,2k,4k+4,6k+6)$ [1, 8, 35]. Remarkably enough, sequentially un-Higgsing $SU(r)$ factors ($r=2,\cdots,4$) leads to Hodge numbers that also match into those of known $K3$ fibrations [8]. The chain of spaces thus

obtained is shown in Table 2.1. Each element is then presumably equivalent to a heterotic $K3 \times T^2$ compactification in which the gauge group can be enhanced to

$$G = SU(r) \times G_2^{(0)}(k) \tag{2.12}$$

at special points in the heterotic moduli space. Indeed, it has been shown [10] that such enhanced groups can also appear in the conjectured type II dual compactification. In fact since the toroidal $U(1)^2$ can be enhanced to $SU(3)$ there can be overall enhancement to a group contained in $G \times SU(3)$.

r	Calabi–Yau Manifold	$K3$
4	$\mathbb{P}_5{}^{(1,1,2k,2k+4,2k+6,2k+8)}[4k+8, 4k+12]$	$\mathbb{P}_4{}^{(1,k,k+2,k+3,k+4)}[2k+4, 2k+6]$
3	$\mathbb{P}_4{}^{(1,1,2k,2k+4,2k+6)}[\ 6k+12]$	$\mathbb{P}_3{}^{(1,k,\ k+2,\ k+3)}[3k+6]$
2	$\mathbb{P}_4{}^{(1,1,2k,2k+4,4k+6)}[\ 8k+12]$	$\mathbb{P}_3{}^{(1,k,\ k+2,2k+3)}[4k+6]$
1	$\mathbb{P}_4{}^{(1,1,2k,4k+4,6k+6)}[12k+12]$	$\mathbb{P}_3{}^{(1,k,2k+2,3k+3)}[6k+6]$

Table 2.1: The k'th chain of hypersurfaces with enhanced group $SU(r) \times G_2^{(0)}(k)$, $k = 1, \cdots, 6$.

The case $k = 5$ is special in that the chain of hypersurfaces do not in fact correspond to heterotic models of the type we have described since this would require $d_2 = 2 < 4$. Moreover, these hypersurfaces do not appear in the lists [14] of Calabi–Yau spaces in weighted $\mathbb{P}_4$ owing to the fact that the weights do not allow for transverse polynomials. This second objection is, however, easily dealt with. It is possible to give meaning to the manifolds of this chain in virtue of the correspondence between Calabi–Yau manifolds and reflexive polyhedra that is provided by the construction of Batyrev [18] in terms of reflexive polyhedra and it is therefore tempting to include this chain here. As for the first objection, we shall see in the next section, that the structure of the $K3$ polyhedra in the $k = 5$ chain is identical to that in the $k = 6$ chain. This strongly suggests that the terminal group is $G_2^{(0)}(5) = E_8$. This proposal works if we modify the $N = 1,\ D = 6$ construction so as to include effects seen in the compactification of M-theory[40, 41, 32, 33] and F-theory [36,35]. More precisely we consider vacua with n_T tensor multiplets so that the condition $d_1 + d_2 = 24$ is replaced by

$$d_1 + d_2 + n_T - 1 = 24\ . \tag{2.13}$$

We immediately see that $n_T = 3$ permits $d_1 = 22,\ d_2 = 0$. In this way we can have a $k = 5$ chain. Moreover, the initial gauge group $E_7 \times E_8$ can be completely broken to a matter-free E_8.

The expressions for h_{11} and h_{12} must be modified since owing to the tensor multiplets, eq. (2.4) becomes [33]

$$n_H - n_V = 273 - 29 n_T \tag{2.14}$$

and we must also take into account that upon further compactification on T^2 the n_T tensor multiplets give rise to n_T $U(1)$ vector multiplets. The effect is that eqs. (2.9) are now replaced by

$$\begin{aligned} h_{11} &= \operatorname{rank} G_2^{(0)}(k) + n_T + 2 \\ h_{12} &= 272 + \dim G_2^{(0)}(k) - 29 n_T \ . \end{aligned} \tag{2.15}$$

Eqs. (2.10) and (2.11) change accordingly. With $n_T = 3$ and $G_2^{(0)}(5) = E_8$ we recover the observed Hodge numbers of the $k = 5$ spaces.

For $k = 0$ we have a heterotic construction but this value does not admit of a simple interpretation in terms of the manifolds of Table 2.1. However, this interesting case can be analyzed following the approach of ref. [35]. Indeed, it has been pointed out that the terminal hypersurface $\mathbb{P}_4^{(1,1,2k,4k+4,6k+6)}[12k{+}12]$ can also be viewed as an elliptic fibration over the Hirzebruch surface $\mathbb{F}_{2k}$ [35]. As we will explain shortly, in this setting it is natural to consider $k = 0$ as well as $k =$half-integer. We will now briefly discuss the latter situation.

When $k = 1/2$, the second E_7 can be broken completely so that $G_2^{(0)}(1/2) = SU(1)$. When $k = 3/2$, sequential breaking ends in $SU(3)$ [32]. Notice that $\tilde{v}/v = -3/2$ for a matter-free $SU(3)$. When $k = 5/2$ the breaking can proceed to $G_2^{(0)}(5/2) = F_4$ [42]. For a matter-free F_4, $\tilde{v}/v = -5/2$ [39], as expected. When $k = 7/2$, there is no known breaking, the terminal group is just E_7 with a half **56** hypermultiplet. Finally, the values $k = 9/2, 11/2$ require $n_T = 4, 2$ tensor multiplets and since $d_2 = 0$, the terminal group is E_8. This is summarized by Table 2.2.

In general, if G_2 stays completely broken at a matter free $G_2^{(0)}(k)$ and considering different $G_1 \to H$ breaking patterns leads to models with Hodge numbers of the form

$$\begin{aligned} h_{11} &= \operatorname{rank} G_2^{(0)}(k) + \operatorname{rank} H + n_T(k) + 2 \\ h_{21} &= 272 + \dim G_2^{(0)}(k) + \dim H - 29 n_T(k) - a_H - b_H k \ . \end{aligned} \tag{2.16}$$

The coefficients a_H and b_H encode the number of H-charged fields that disappear in the Coulomb phase, their values are recorded in Table 3.2 for a number of groups that we

shall meet. Although $SO(12)$ cannot be obtained from E_7 by the usual Higgs mechanism, it arises naturally from breaking of the original E_8 by background $SU(2) \times SU(2)$ fields with total instanton number $d_1 = 12 + 2k$. For $SU(6)$ we have considered the two simplest possibilities with $\tilde{v}/v = k$. For $SU(6)$, $n_6 = 16 + 4k$, $n_{15} = 2k + 2$ and $n_{20} = 0$, whereas for $SU(6)_b$, $n_6 = 18 + 6k$, $n_{15} = 0$ and $n_{20} = k + 1$ (the **20** is a pseudoreal representation). Each of these cases can be obtained by Higgsing an $SO(12)$ with appropriate numbers of **32**s and **32′**s that in turn depend on how d_1 is distributed between the two $SU(2)$'s [43].

k	0	$\frac{1}{2}$	1	$\frac{3}{2}$	2	$\frac{5}{2}$	3	$\frac{7}{2}$	4	$\frac{9}{2}$	5	$\frac{11}{2}$	6
$G_2^{(0)}$	SU_1	SU_1	SU_1	SU_3	SO_8	F_4	E_6	E_7^-	E_7	E_8	E_8	E_8	E_8
$\mathrm{rk}[G_2^{(0)}]$	0	0	0	2	4	4	6	7	7	8	8	8	8
$\dim[G_2^{(0)}]$	0	0	0	8	28	52	78	105	133	248	248	248	248
n_T	1	1	1	1	1	1	1	1	1	4	3	2	1

Table 2.2: Terminal groups and the numbers of tensor multiplets for the different values of k. The entry E_7^- corresponding to $k = \frac{7}{2}$ denotes E_7 with a half-multiplet of **56**. The entries in this column give the values that are appropriate to the use of the relations (2.16) for this case.

3. **Sequences of Reflexive Polyhedra**

3.1. General structure

We now set out to study the Calabi–Yau spaces conjectured to give the type IIA dual description of the heterotic compactifications explained in the previous section. Our strategy is to analyze the manifolds following Batyrev's toric approach. (For a concise summary of Batyrev's construction in a form accesible to physicists see, for example, [16].) To a Calabi–Yau manifold (of any dimension) defined as a hypersurface in a weighted projective space one can associate its Newton polyhedron, which we denote by Δ. The Newton polyhedron is often (perhaps always) reflexive and when it is we may define the dual or polar polyhedron which we denote by ∇. By means of a computer program we have computed the dual polyhedra for the last three manifolds given in Table 2.1. The polyhedra for each k have similar properties that we will illustrate by considering $k = 1$ as an example. For this case, the points of the dual polyhedra are displayed in Table 3.1. We shall modify these polyhedra shortly so for the present the ∇'s are distinguished by tildes.

${}^4\widetilde{\nabla}^{SU(1)}$	${}^4\widetilde{\nabla}^{SU(2)}$	${}^4\widetilde{\nabla}^{SU(3)}$
$(-1,\ 0,\ 2,\ 3)$	$(-1,\ 0,\ 2,\ 3)$	$(-1,\ 0,\ 2,\ 3)$
$*(\ 0,-1,\ 2,\ 3)$	$*(\ 0,-1,\ 1,\ 2)$	$*(\ 0,-1,\ 1,\ 1)$
$(\ 0,\ 0,-1,\ 0)$	$(\ 0,\ 0,-1,\ 0)$	$(\ 0,\ 0,-1,\ 0)$
$(\ 0,\ 0,\ 0,-1)$	$(\ 0,\ 0,\ 0,-1)$	$(\ 0,\ 0,\ 0,-1)$
$(\ 0,\ 0,\ 0,\ 0)$	$(\ 0,\ 0,\ 0,\ 0)$	$(\ 0,\ 0,\ 0,\ 0)$
$(\ 0,\ 0,\ 0,\ 1)$	$(\ 0,\ 0,\ 0,\ 1)$	$(\ 0,\ 0,\ 0,\ 1)$
$(\ 0,\ 0,\ 1,\ 1)$	$(\ 0,\ 0,\ 1,\ 1)$	$(\ 0,\ 0,\ 1,\ 1)$
$(\ 0,\ 0,\ 1,\ 2)$	$(\ 0,\ 0,\ 1,\ 2)$	$(\ 0,\ 0,\ 1,\ 2)$
$(\ 0,\ 0,\ 2,\ 3)$	$(\ 0,\ 0,\ 2,\ 3)$	$(\ 0,\ 0,\ 2,\ 3)$
$(\ 0,\ 1,\ 2,\ 3)$	$(\ 0,\ 1,\ 2,\ 3)$	$(\ 0,\ 1,\ 2,\ 3)$
$(\ 1,\ 2,\ 2,\ 3)$	$(\ 1,\ 2,\ 2,\ 3)$	$(\ 1,\ 2,\ 2,\ 3)$

Table 3.1: The dual polyhedra for $k = 1$ and $H = SU(1)$, $SU(2)$ and $SU(3)$.

The following observations summarize the structure of the polyhedra:

1. For each polyhedron all the points except two (the first and the last) lie in the hyperplane $x_1 = 0$. In each case the points that lie in the hyperplane $x_1 = 0$ themselves form a reflexive polyhedron which is the dual of the polyhedron for the respective $K3$ of the fibration.

2. Omitting the first two points and the last two points of each polyhedron leaves us with a two-dimensional reflexive polyhedron, ${}^2\nabla$, which is a triangle. This ${}^2\nabla$ is the dual polyhedron of the torus $\mathbb{P}_2{}^{(1,2,3)}$[6]. We see in this way that the $K3$'s are elliptically fibred as elucidated in ref. [35]

3. The three polyhedra of Table 3.1 differ only in the second point of each (which is distinguished by an asterisk). Let δ denote the (non-reflexive) polyhedron consisting of the common points and denote by $pt'_r,\ r = 1, 2, 3$, the three special points $pt'_1 = (0, -1, 2, 3)$, $pt'_2 = (0, -1, 1, 2)$ and $pt'_3 = (0, -1, 1, 1)$ (the utility of the primes will become apparent as we proceed). Then we have

$$ {}^4\widetilde{\nabla}^{SU(r)} = \delta \cup pt'_r \ . $$

   We observe that we can add points to the polyhedra as follows without changing the Hodge numbers of the associated manifolds.

$$ \begin{aligned} {}^4\nabla^{SU(1)} &= {}^4\widetilde{\nabla}^{SU(1)} \\ {}^4\nabla^{SU(2)} &= {}^4\widetilde{\nabla}^{SU(2)} \cup pt'_1 \\ {}^4\nabla^{SU(3)} &= {}^4\widetilde{\nabla}^{SU(3)} \cup pt'_1 \cup pt'_2 \end{aligned} $$

   The fact that the Hodge numbers of ${}^4\nabla^{SU(r)}$ and ${}^4\widetilde{\nabla}^{SU(r)}$ are the same may mean that the polyhedra correspond to the same manifold. However, whether this is or not the case, we will take the sequence of polyhedra on the left of these relations as defining the chain, abandoning if need be the sequence of spaces of Table 2.1 that was our original motivation.

4. The pt'_r lie in the hyperplane $x_1 = 0$ and the observation above that the points of the polyhedra that lie in the hyperplane $x_1 = 0$ form a reflexive polyhedron continues to hold for the augmented polyhedra ${}^4\nabla^{SU(r)}$. We are therefore dealing with a succession of $K3$ manifolds and the relations above hold equally well if each ${}^4\nabla$ is replaced by a ${}^3\nabla$ referring to the $K3$'s.

5. Fix attention now on the polyhedra, ${}^3\nabla$, of the $K3$'s and the two dimensional polyhedron, ${}^2\nabla$, of the torus. The ${}^2\nabla$ is the same for each of the three spaces. It consists

of the 7 points that have $x_1 = x_2 = 0$. ${}^2\nabla$ divides ${}^3\nabla$ into a 'top', ${}^3\nabla_{\rm top}$, consisting of points for which $x_1 = 0$ and $x_2 \geq 0$ and a 'bottom', ${}^3\nabla_{\rm bot}$, consisting of points for which $x_1 = 0$ and $x_2 \leq 0$. Figure 3.1 illustrates this for the case $k = 3$ and $r = 3$. As we move up the chain ${}^3\nabla_{\rm bot}$ changes, it is succesively

$$ {}^2\nabla \cup pt'_1 \rightarrow {}^2\nabla \cup pt'_1 \cup pt'_2 \rightarrow {}^2\nabla \cup pt'_1 \cup pt'_2 \cup pt'_3 \rightarrow \cdots \ . \tag{3.1} $$

The polyhedron ${}^3\nabla_{\rm top}$ however is unchanged as we move up the chain.

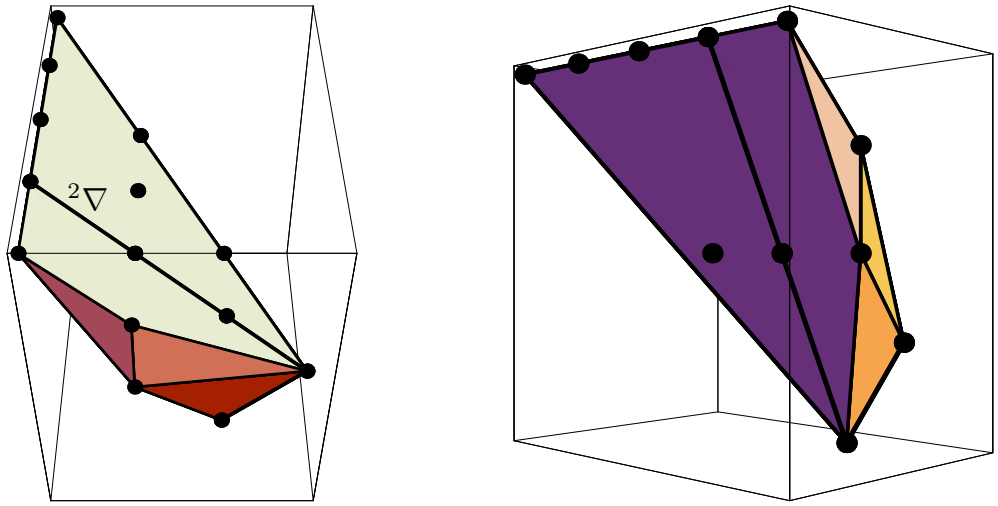

Figure 3.1: Two views of the polyhedron ${}^3\nabla^{k=3,\,SU(3)}$. The polyhedron is divided into a top and a bottom by the triangle ${}^2\nabla$.

We can now elaborate on our statement that for each chain a similar pattern obtains. Apart from two points, which for each member of the k'th chain are $(-1, 0, 2, 3)$ and $(1, 2k, 2, 3)$, the points of the polyhedron lie in the plane $x_1 = 0$ forming the polyhedron, ${}^3\nabla$, of the $K3$. For each member of a chain, the polyhedron of the $K3$ is again divided into a top and a bottom by the polyhedron ${}^2\nabla$ of the torus and we may write

$$ {}^3\nabla^{k,H} = \nabla^H_{\rm bot} \cup \nabla^k_{\rm top} \ , \tag{3.2} $$

where $\nabla^k_{\rm top}$ depends only on k while $\nabla^H_{\rm bot}$ depends only on the group H that is perturbatively restored in the heterotic side. In particular then, the dual polyhedron ${}^4\nabla^{k,SU(1)}$

of the lowest space $\mathbb{P}_4{}^{(1,1,2k,4k+4,6k+6)}[12k+12]$ can be written as

$$ {}^4\nabla^{k,SU(1)} = {}^3\nabla^{k,SU(1)} \cup \{(-1,0,2,3),\ (1,2k,2,3)\}\ . \tag{3.3} $$

We can describe the tops and bottoms of ${}^3\nabla^{k,H}$ quite simply. If we denote by $\mathcal{T}^k$ the tetrahedron with base ${}^2\nabla$ and top vertex $(0,k,2,3)$, the top polyhedron may be specified as follows:

$$ \begin{aligned} \nabla^k_{\rm top} &= \mathcal{T}^k\ , \quad \text{for } k=1,2,3 \\ \nabla^4_{\rm top} &= \mathcal{T}^4 \cup \{(0,1,0,0),\ (0,2,0,1),\ (0,3,1,2)\} \\ \nabla^5_{\rm top} &= \nabla^6_{\rm top} = \mathcal{T}^6\ . \end{aligned} $$

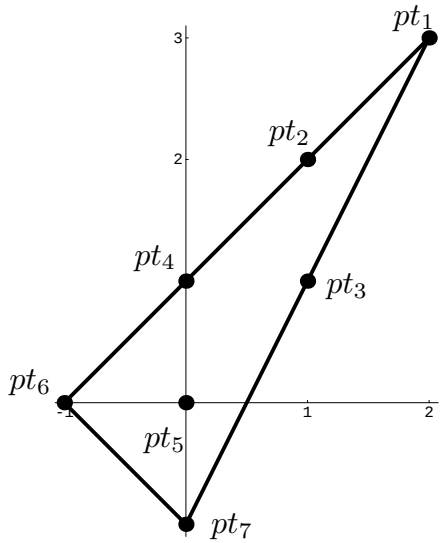

Figure 3.2: The polyhedron, ${}^2\nabla$, of $\mathbb{P}_2{}^{(1,2,3)}[6]$. The pt'_r are the points directly below the indicated points of the plot.

We can also easily describe $\nabla^H_{\rm bot}$ for $H = SU(r)$, $r = 1,2,3$. Consider first the polyhedron ${}^2\nabla$ shown in Figure 3.2 and let pt'_r be, as previously, the points of the lattice that are directly below the corresponding points of ${}^2\nabla$. We find that

$$ \nabla^{SU(r)}_{\rm bot} = {}^2\nabla \cup \bigcup_{j=1}^{r} pt'_j\ . \tag{3.4} $$

H	Bottom	a_H	b_H	$\tilde{n}_T$
$SU(1)$	$\{pt'_1\}$	0	0	n_T
$SU(2)$	$\{pt'_1, pt'_2\}$	32	24	n_T
$SU(3)$	$\{pt'_1, pt'_2, pt'_3\}$	54	36	n_T
G_2	$\{pt''_1, pt'_2, pt'_3\}$	60	36	n_T
$SO(5)$	$\{pt'_1, pt'_2, pt'_4\}$	68	40	n_T
$SU(4)$	$\{pt'_1, pt'_2, pt'_3, pt'_4\}$	76	44	n_T
$SO(7)$	$\{pt''_1, pt'_2, pt'_3, pt'_4\}$	82	44	n_T
Sp_3	$\{pt'_1, pt'_2, pt'_4, pt'_6\}$	108	48	n_T
$SU(5)$	$\{pt'_1, pt'_2, pt'_3, pt'_4, pt'_5\}$	100	50	n_T
$SO(9)$	$\{pt''_1, pt''_2, pt'_3, pt'_4\}$	104	48	n_T
F_4	$\{pt'''_1, pt''_2, pt'_3, pt'_4\}$	120	48	n_T
$SU(6)$	$\{pt'_1, pt'_2, pt'_3, pt'_4, pt'_5, pt'_6\}$	126	54	n_T
$SU(6)_b$	$\{pt'_1, pt'_2, pt'_3, pt'_4, pt'_5, pt'_7\}$	128	56	n_T
$SO(10)$	$\{pt''_1, pt''_2, pt'_3, pt'_4, pt'_5\}$	124	52	n_T
$SO(11)$	$\{pt''_1, pt''_2, pt'_3, pt''_4, pt'_5\}$	134	52	n_T
$SO(12)$	$\{pt''_1, pt''_2, pt'_3, pt''_4, pt'_5, pt'_6\}$	160	56	n_T
E_6	$\{pt'''_1, pt''_2, pt''_3, pt'_4, pt'_5\}$	162	54	n_T
E_7	$\{pt''''_1, pt'''_2, pt''_3, pt''_4, pt'_5\}$	224	56	n_T
$SU(6)_c$	$\{pt'_1, pt'_2, pt'_3, pt'_4, pt'_5, pt'_6, pt'_7\}$	72	0	$n_T + 2k + 2$
$SO(13)$	$\{pt''_1, pt''_2, pt'_3, pt''_4, pt'_5, pt''_6\}$	60	0	$n_T + 2k + 4$
E_{6B}	$\{pt'''_1, pt''_2, pt''_3, pt'_4, pt'_5, pt'_7\}$	0	0	$n_T + 2k + 6$
E_{7B}	$\{pt''''_1, pt'''_2, pt''_3, pt''_4, pt'_5, pt'_6\}$	0	0	$n_T + 2k + 8$
E_8	$\{pt^{(6)}_1, pt^{(4)}_2, pt'''_3, pt''_4, pt'_5\}$	0	0	$n_T + 2k + 12$

Table 3.2: The bottoms containing pt'_1 formed by adding the points $pt_r^{(j)}$ to ${}^2\nabla$. In each case the points of ${}^2\nabla$ are understood and the points that are written are the lowest members of columns. Thus pt'''_2 for example implies the presence of pt''_2 and pt'_2. The bottoms that appear in the lower block correspond to nonperturbatively realised groups. The coefficients a_H and b_H, on the right, are the quantities that appear in the expressions (2.16) for the Hodge numbers. The quantity $\tilde{n}_T$ denotes the number of tensor multiplets while n_T refers to the quantities given by the third row of Table 2.2.

H	Bottom	a_H	b_H	$\tilde{n_T}$
$SU(2)_b$	$\{pt'_2\}$	32	24	n_T
$SU(2)_c$	$\{pt'_4\}$	62	36	n_T
$SU(2)_d$	$\{pt'_6\}$	92	36	n_T
$SU(2) \times SU(2)$	$\{pt'_2, pt'_4\}$	64	40	n_T
$(SU(2) \times SU(2))_b$	$\{pt'_4, pt'_6\}$	94	44	n_T
$SU(3) \times SU(2)$	$\{pt'_2, pt'_4, pt'_5\}$	86	48	n_T
$(SU(3) \times SU(2))_b$	$\{pt'_3, pt'_5\}$	86	48	n_T
$(SU(3) \times SU(2))_c$	$\{pt'_5\}$	86	48	n_T
$SO(5) \times SU(2)$	$\{pt'_2, pt'_4, pt'_6\}$	100	48	n_T
$G_2 \times SU(2)$	$\{pt'_2, pt''_4, pt'_5\}$	92	48	n_T
$SU(4) \times SU(2)$	$\{pt'_2, pt'_4, pt'_5, pt'_6\}$	108	52	n_T
$SO(7) \times SU(2)$	$\{pt'_2, pt''_4, pt'_5, pt'_6\}$	114	52	n_T
$SO(9) \times SU(2)$	$\{pt'_2, pt''_4, pt'_5, pt''_6\}$	136	56	n_T
$SU(3)_b$	$\{pt'_3\}$	54	36	n_T
$SU(3)_c$	$\{pt'_7\}$	102	48	n_T
$SU(3) \times SU(3)$	$\{pt'_3, pt'_5, pt'_7\}$	108	54	n_T
$G_2 \times SU(3)$	$\{pt'_3, pt'_5, pt''_7\}$	114	0	$n_T + 2k$
$F_4 \times SU(2)$	$\{pt'_2, pt''_4, pt'_5, pt'''_6\}$	152	0	$n_T + 2k$

Table 3.3: The bottoms that do not contain pt'_1. The bottoms that are given in the lower block again correspond to groups that are realised nonperturbatively.

Moreover, we have verified that including the point $pt'_4 = (0, -1, 0, 1)$ leads to a reflexive polyhedron that gives the expected Hodge numbers for an enhanced $SU(4)$. Further adding $pt'_5 = (0, -1, 0, 0)$ corresponds to an enhanced $SU(5)$ and $pt'_6 = (0, -1, -1, 0)$ to an enhanced $SU(6)$. Hence, eq. (3.4) is actually valid for $r = 1, \cdots, 6$. Note that we are abandoning the $SU(4)$ manifolds of Table 2.1 in favour of the definition that we are giving here. It would be of interest to see if these manifolds are in fact the same.

We denote by pt''_r the point that is two levels vertically below pt_r and more generally by $pt_r^{(j)}$ the point that is j levels below. We consider now the possibility of adding com-

binations of the points $pt_i^{(j)}$ in all possible ways such that the bottom corresponds to a reflexive polyhedron that contains pt'_1. This is straightforward in virtue of the fact that if the polyhedron is to be reflexive the point pt'_5 cannot be interior to the polyhedron. Since the polyhedra must be convex we can at most drop down 6 levels below pt_1, 4 below pt_2, 3 below pt_3, 2 below pt_4, 1 below pt_5 and 2 below each of pt_6 and pt_7. Very few of the possible combinations lead to convex polyhedra. We have enumerated all the combinations of points that do. Table 3.2 shows the allowed bottoms leading to reflexive polyhedra that correspond to enhanced gauge groups $H \times G_2^{(0)}(k)$. The resulting Hodge numbers, recorded in Tables A.1 and A.2 in the Appendix, can be seen to agree with (2.16).

All the groups obtained by the sequential Higgsing (2.2) do appear and, as a matter of consistency, we see the inclusions

$$E_7 \supset E_6 \supset SO(10) \supset SU(5) \supset SU(4) \supset SU(3) \supset SU(2) \supset SU(1) \ ,$$

as inclusions of the respective polyhedra. We also observe that $SO(10) \supset SO(8) \supset SU(4) \supset SU(2)^2$ as expected from Higgsing. Likewise, there are bottoms corresponding to $SO(12) \supset SU(6) \supset SU(2)^3$ that contain pt'_6 which is not a point of the E_7 polyhedron. Finally, only the bottom for $SU(6)_b$ contains pt'_7. Clearly $SU(6)_b \supset SU(5)$. The fact that $SO(12) \not\supset SU(6)_b$ suggests that the matter content of this $SO(12)$ does not include **32**s that could give rise to the **20**s present in $SU(6)_b$.

The rest of the bottoms giving reflexive polyhedra are presented in the lower block of Table 3.2. Before discussing their interpretation, which involves non-perturbative effects, we describe the extension of the previous analysis to the remaining values of k.

3.2. $k = 0$ and $k =$ half integer

We wish to consider also the cases for which $k = 0$ and $k =$ half-integer. It is simplest to discuss first the cases $k = \frac{3}{2}, \frac{5}{2}, \ldots, \frac{11}{2}$. For these cases the manifolds in the left hand column of Table 2.1 still make sense though the $K3$-fibration is less easy to see. On constructing the duals of the Newton polyhedra we find that precisely the same structure emerges as for the case of k integral. In particular all points except two lie in a plane and these points form the polyhedron, ${}^3\nabla$, of a $K3$. This shows that the manifolds are indeed $K3$-fibrations with generic fiber corresponding to the polyhedron ${}^3\nabla$. Again each ${}^3\nabla$ contains a ${}^2\nabla$ which divides the ${}^3\nabla$'s into tops and bottoms with the bottoms independent of k.

For $k = 0$ the manifolds of Table 2.1 make no sense since the weight of the third coordinate would be zero. While for $k = \frac{1}{2}$ the lowest member of the chain would be $\mathbb{P}_4{}^{(1,1,1,6,9)}[18]$ which is not a $K3$-fibration. The cases $k = 0$ and $k = \frac{1}{2}$ are however covered by a construction of Morrison and Vafa [35] which realizes the lowest member of each chain as an elliptic fibration over the Hirzebruch surface $\mathbb{F}_{2k}$. Each manifold is described as a space of seven complex variables s, t, u, v, x, y, z subject to three scaling symmetries with parameters λ, μ, ν. The variables scale with weights shown in Table 3.4.

	s	t	u	v	x	y	z	degrees
λ	1	1	$2k$	0	$4k$+4	$6k$+6	0	$12k + 12$
μ	0	0	1	1	4	6	0	12
ν	0	0	0	0	2	3	1	6

Table 3.4: The scaling weights of the elliptic fibration over $\mathbb{F}_{2k}$.

The Newton Polyhedron of the Calabi–Yau manifold defined by the data in Table 3.4 is constructed by finding all possible monomials $s^{m_1}t^{m_2}u^{m_3}v^{m_4}x^{m_5}y^{m_6}z^{m_7}$ whose degrees under the three scalings are given by the right hand column of the Table. Owing to the three constraints on the seven exponents, $m_1, \ldots, m_7$, the allowed monomials lie in a four-dimensional lattice within $\mathbb{R}^7$. The convex hull of the monomials is the Newton polyhedron. The polyhedron contains the point $(1, 1, 1, 1, 1, 1, 1)$, corresponding to the monomial $stuvxyz$, as its only interior point. By translating the origin to this point, constructing the dual polyhedron and making a $GL(4, \mathbb{Z})$ transformation we obtain, in all cases, polyhedra that are exactly of the form given in (3.3). The form of the various $\nabla^k_{\rm top}$'s is given in Tables 3.5 where the tops for all k are included for puposes of comparison. For $k = 0$ the construction yields a space that is best thought of as an elliptic fibration over $\mathbb{F}_0 = \mathbb{P}_1 \times \mathbb{P}_1$. For $k = \frac{1}{2}$ the construction yields a space that differs from $\mathbb{P}_4{}^{(1,1,1,6,9)}[18]$ owing to the presence of an extra constraint. In all other cases it is easy to see that this construction gives again the space $\mathbb{P}_4{}^{(1,1,2k,4k+4,6k+6)}[12k+12]$.

The point of view that we adopt here is that the polyhedron picture is to be preferred over the chains of projective spaces that were studied by Aldazabal it et al.[8]. We have already seen that points can sometimes be added to the polyhedron without changing the Hodge numbers that were the basis for the identifications and that when this is done the polyhedra can be seen to fall into a regular sequence. This proves to be true of the tops

k	$\nabla^k_{\rm top}$
0, $\frac{1}{2}$, 1	$\mathcal{T}^1$
$\frac{3}{2}$	$\mathcal{T}^1 \cup (0,1,1,2)$
2	$\mathcal{T}^2$
$\frac{5}{2}$, 3	$\mathcal{T}^3$
$\frac{7}{2}$, 4	$\mathcal{T}^4 \cup \{(0,1,0,0),\ (0,2,0,1),\ (0,3,1,2)\}$
$\frac{9}{2}$, 5, $\frac{11}{2}$, 6	$\mathcal{T}^6$

Table 3.5: The tops for each of the chains with $k = 0, \frac{1}{2}, \ldots, 6$.

also and we will return after understanding the structure of the bottoms to cast the tops in their final form.

The polyhedra corresponding to restored gauge symmetries are constructed, as explained previously, by leaving the tops alone and modifying the bottoms according to Table 3.2. In this way we obtain Hodge numbers in agreement with what we expect on the basis of the dual heterotic picture. The Hodge numbers recorded in Tables A.1 and A.2 of the appendix have been computed directly from the polyhedra and can be seen to agree with eq. (2.16) for $k = 0, 1/2, \cdots, 6$.

3.3. Non-perturbative effects

We have seen that symmetry restoration in a terminal heterotic model can be interpreted as adding points in the ${}^4\nabla_{\rm bot}$ piece of ${}^4\nabla^k$, or equivalently, as imposing certain additional conditions on the monomial deformations that determine the dual Newton polyhedron. Notice that in this process, the $K3$ fibers are modified. We have then a qualitative explanation of our results since, as explained by Aspinwall [10], the actual non-Abelian structure of the group that is perturbatively visible is related in turn to the structure of the $K3$ fibers. The arguments of refs. [9,10,38] also provide some hints for how to look for gauge groups that cannot be seen perturbatively. The basic idea is to include the effect of degenerate fibers or to modify the $\mathbb{P}_1$ part of the fibration. Some of this can be done torically and amounts to adding points outside the plane of the $K3$.

Motivated by the shape of ${}^4\nabla^{k,SU(1)}$, we have noticed that adding points $(1, 2k-j, 2, 3)$, $j = 1, \cdots, 2k+2$ to this polyhedron is always consistent with reflexivity. Moreover, the Hodge numbers in this new sequence of polyhedra have a rather interesting pattern as we now describe. The transitions along the new branch are characterized by

$$\Delta h_{12} = -29 \qquad ; \qquad \Delta h_{11} = 1 \ . \tag{3.5}$$

Hence, as implied by eq. (2.14), they can be explained as transitions in which $n_T \to n_T + 1$. Since, eq. (2.13) requires $(d_1 + d_2) \to (d_1 + d_2 - 1)$, this corresponds to shrinking of an instanton [32, 33]. The result (3.5) is consistent with $d_1 \to d_1 - 1$ while d_2 is kept fixed. The first E_7 can be completely broken for $d_1 \geq 10$ so that to arrive at $SU(1)$ the original $d_1 = 12 + 2k$ can only be decreased in one unit $2 + 2k$ times as we have observed.

The new sequence of polyhedra has then a non-perturbative interpretation. The observed transitions are dual to some heterotic dynamics that can only be seen in M-theory. The result (3.5) is also compatible with un-Higgsing of a non-perturbative $SU(2)$ accompanied by exactly 16 doublets. When $k = 0$, eq. (2.6) shows that un-Higgsing of a *perturbative* $SU(2)$ precisely comes together with 16 doublets. Thus, in this case, the same group structure can appear along the perturbative and non-perturbative branches. Similar results were noticed in ref. [32] for the heterotic vacuum and in ref. [38] for the type II vacuum. In our approach this is manifest given the $\mathbb{Z}_2$ symmetry $x_1 \leftrightarrow x_2$ of the $k = 0$ polyhedron (3.3) that corresponds to exchange of the $\mathbb{P}_1$'s in $\mathbb{F}_0 = \mathbb{P}_1 \times \mathbb{P}_1$. Thus, adding points $\widetilde{pt}_i^{(j)}$ obtained from $pt_i^{(j)}$ by $x_1 \leftrightarrow x_2$ leads to the same perturbative groups but with a non-perturbative interpretation since we have left fixed the generic $K3$ fiber.

We have also considered the effect of adding sequentially the points $(1, 2k-j, 2, 3)$ for $j = 1, 2, \ldots$, to the polyhedron ${}^4\nabla^{H,k}$ for all the H that we have identified. For $j \leq j_H$, with j_H an upper bound depending on H, this always leads to a reflexive polyhedron and the Hodge numbers for these sequences also have an interesting pattern. To be more precise, we denote by $\nabla^{H,k,j}$ the augmented polyhedron:

$$\nabla^{H,k,j} = {}^4\nabla^{H,k} \cup \big\{(1, 2k-1, 2, 3),\ (1, 2k-2, 2, 3),\ \ldots,\ (1, 2k-j, 2, 3)\big\}$$

The extra points are being added to the two-face of ${}^4\nabla^{H,k}$ given by $x_3 = 2$ and $x_4 = 3$. Consider now the Hodge numbers of $\nabla^{H,k,j}$ which, of course, depend on (H, k, j). If we fix H and k and consider the differences, $(\Delta h_{11}, \Delta h_{21})$, between $\nabla^{H,k,j+1}$ and $\nabla^{H,k,j}$ then these differences are observed to be independent of k and of j for $0 \leq j \leq j_H$, and hence depend only on the group H. Specifically, by an enumeration of cases, we find

$$\Delta h_{12} = -29 + \frac{1}{2} b_H \ , \quad \Delta h_{11} = 1 \ , \tag{3.6}$$

where the coefficients b_H are those given in Table 3.2. Our interpretation is that the transitions $\nabla^{H,k,j} \to \nabla^{H,k,j+1}$ correspond to processes in which

$$n_T \to n_T + 1 \ , \qquad d_1 \to d_1 - 1$$

and d_2 is kept fixed. The term proportional to b_H in h_{12} arises because the decrease in d_1 effectively implies $k \to k - \frac{1}{2}$. The bound j_H depends on the values of d_1 that allow breaking to H. This can be determined by looking at the number of fields in the various representations and the breaking patterns. In this way we obtain results that agree with the observed values of j_H obtained from the polyhedra by continuing the sequence $\nabla^{H,k,j}$ until the polyhedra cease to be reflexive.

Non-perturbative effects related to changes in the number of tensor multiplets also provide an interpretation of the remaining reflexive polyhedra obtained by systematically enlarging the bottoms as explained in section 3.1. In all the cases in the lower block of Table 3.2, the Hodge numbers computed from the polyhedra take the form

$$\begin{aligned} h_{11} &= \operatorname{rank} G_2^{(0)}(k) + \operatorname{rank} H + \tilde{n}_T + 2 \\ h_{21} &= 272 + \dim G_2^{(0)}(k) + \dim H - 29\tilde{n}_T - a_H - b_H \tilde{k} \ . \end{aligned} \tag{3.7}$$

where $\tilde{n}_T$ is given in Table 3.2 and $\tilde{k} = \frac{1}{2}(2k + n_T(k) - \tilde{n}_T)$. If we define $\tilde{d}_1 = 12 + 2\tilde{k}$, the enlarged polyhedra then appear to correspond to heterotic compactifications with instanton numbers $(\tilde{d}_1, d_2)$, $\tilde{n}_T$ tensor multiplets and an enhanced group $H \times G_2^{(0)}(k)$. For example, when $H = E_8$ with $\tilde{k} = -6$ and $k = \frac{9}{2}$, 5, $\frac{11}{2}$, 6, the enhanced group is $E_8 \times E_8$, with $\tilde{d}_1 = d_2 = 0$ and $\tilde{n}_T = 25$. The Hodge numbers obtained from (3.7), $h_{11} = h_{21} = 43$, are characteristic of a compactification with 25 tensor multiplets[33, 44]. Note that $b_H = 0$ in all these cases, reflecting the fact that $\tilde{d}_1$ is independent of $\tilde{k}$ and hence, so is the H charged matter content.

3.4. Irreducibility

It is of interest to examine whether the $\nabla^{SU(1),k}$ polyhedra corresponding to the terminal groups of each chain are irreducible [25,26]. It seems that this should be so since it is not possible to break the symmetry further. Thus the irreducibility of the polyhedra is a consistency check on duality and the identity of the webs. By irreducible here we mean torically irreducible. That is there is no reflexive sub-polyhedron of the given polyhedron. There is a stricter notion of irreducibility which is more appropriate which is that the

given manifold contains no (complex) curves that can be blown down without violating the condition $c_1 = 0$. Thus it is possible for a manifold to be reducible but to be torically irreducible. Of course if a manifold is irreducible in the strict sense it must also be torically irreducible. Thus the toric irreducibility of the manifolds is a consistency check on duality though a weaker one than veryfying irreducibility in the strict sense.

In virtue of the simple structure of the polyhedra the question of the toric irreducibility of the terminal manifolds of the chains can be examined quite simply. Consider the terminal model of the k'th chain. This has the points:

$$\begin{array}{ll}
*(-1,\ 0,\ 2,\ 3) & (\ 0,\ 0,\ 1,\ 1) \\
*(\ 0,-1,\ 2,\ 3) & (\ 0,\ 0,\ 1,\ 2) \\
*(\ 0,\ 0,-1,\ 0) & (\ 0,\ 0,\ 2,\ 3) \\
*(\ 0,\ 0,\ 0,-1) & (\ 0,\ 1,\ 2,\ 3) \\
(\ 0,\ 0,\ 0,\ 0) & \vdots \qquad\quad \vdots \\
(\ 0,\ 0,\ 0,\ 1) & *(\ 1,2k,\ 2,\ 3)\ .
\end{array}$$

In this list we have distinguished by asterisks five points which cannot be discarded if we are to find a reflexive sub-polyhedron. The first point of the list is the only one with $x_1 < 0$. This point cannot be omitted since then the origin would lie in a face. This point is also a vertex. Similarly the last point is the only one with $x_1 > 0$ and cannot therefore be omitted and is also a vertex. The second, third and fourth points are the only ones that have negative entries in the second, third and fourth columns respectively so these points must also be retained and are also vertices. Since we have to retain these five points we must retain also their convex hull. We can show now that this contains the tetrahedron $\mathcal{T}^k$. The third and fourth points of ${}^4\nabla^k$ are vertices of ${}^2\nabla$. The third vertex of ${}^2\nabla$ is

$$(\ 0,\ \ 0,\ \ 2,\ \ 3) = \frac{1}{2k+2}\big\{(-1,\ \ 0,\ \ 2,\ \ 3) + (\ 1,2k,\ \ 2,\ \ 3) + 2k(\ 0,\ \ 1,\ \ 2,\ \ 3)\big\}$$

and is therefore a point of the convex hull as is

$$(\ 0,\ \ k,\ \ 2,\ \ 3) = \frac{1}{2}\big\{(-1,\ \ 0,\ \ 2,\ \ 3) + (\ 1,2k,\ \ 2,\ \ 3)\big\}$$

which is the top vertex of $\mathcal{T}^k$.

For some of the polyhedra the above observations already show that the convex hull contains the entire polyhedron which is therefore irreducible. For the remaining cases the only points that could perhaps be omitted are subsets of ${}^3\nabla^k_{\rm top} \setminus \mathcal{T}^k$. An enumeration

of possibilities, however, shows that all the polyhedra are irreducible except for the single case of the $k = \frac{1}{2}$ polyhedron for which it is possible to omit the point $(0, 1, 2, 3)$ which, in this case, is a vertex. The resulting polyhedron is the dual of the Newton polyhedron of $\mathbb{P}_4{}^{(1,1,1,6,9)}[18]$. This manifold is not a $K3$-fibration so for the case $k = \frac{1}{2}$ the polyhedron is irreducible in the weaker sense that it contains no reflexive subpolyhedron that is a $K3$-fibration.

A final remark is perhaps in order. While there is no minimal polyhedron that is contained in all the polyhedra that we have discussed it would be of interest to know if there is a maximal polyhedron. We do not know if this is the case. However if we denote by ${}^3\widehat{\nabla}^6_{\rm top}$ the bottom formed by reflecting ${}^3\nabla^6_{\rm top}$ in ${}^2\nabla$ (this is in fact the bottom $\{pt_1^{(6)}, \ldots, pt_5'\}$, corresponding to the group E_8, from Table 3.2) then the polyhedron

$$(-1,\ \ 0,\ \ 2,\ \ 3)$$

$$(\ \ 1,\ 12,\ \ 2,\ \ 3)\ ,\ \ (\ \ 1,\ 11,\ \ 2,\ \ 3)\ , \ldots ,\ (\ \ 1, -11,\ \ 2,\ \ 3)\ ,\ \ (\ \ 1, -12,\ \ 2,\ \ 3)$$

$${}^3\nabla^6_{\rm top}\ ,\quad {}^3\widehat{\nabla}^6_{\rm top}$$

is a reflexive elliptic $K3$ fibration and contains all the polyhedra that do not contain pt_6' or pt_7'.

3.5. The final form of the polyhedra and the Dynkin diagrams

In an earlier version of this paper the groups corresponding to the reflexive polyhedra were identified on the basis of their hodge numbers. This led, in some cases, to incorrect identifications and ambiguities owing to the fact that a knowledge of the Hodge numbers alone does not always identify the group uniquely. Thus manifolds corresponding to the groups $SO(8)$, $SO(9)$ and F_4, for example, have the same Hodge numbers as do $SU(2)\times SU(2)$ and $SO(5)$. These ambiguities were resolved by Bershadsky *et al.*[45] who were able to identify the groups on the basis of the singularity structure. Once the ambiguity is resolved however a very beautiful fact emerges which is that the Dynkin diagram of the group and also the extended diagram can be read off from the $K3$-polyhedron. To see this it is instructive to recall that the Hodge numbers (h^{11}, h^{21}) of a hypersurface $\mathcal{M}$ of this family may be calculated directly in terms of data derived from the Newton polyhedron. Let $\mathrm{pts}(\Delta)$ denote the number of integral points of Δ and let Δ_r denote the set of r-dimensional faces of Δ. Write also $\mathrm{int}(\theta)$ for the number of integral points interior to a

face, θ, of Δ and define similar quantities with Δ and ∇ interchanged. Duality provides a unique correspondence between an r-dimensional face, θ, of Δ and a $(3-r)$-dimensional face $\tilde{\theta}$ of ∇. With this notation the formulae[46,47] for the Hodge numbers are

$$\begin{aligned} h^{21}(\Delta) &= \mathrm{pts}(\Delta) - \sum_{\theta\in\Delta_3} \mathrm{int}(\theta) + \sum_{\theta\in\Delta_2} \mathrm{int}(\theta)\,\mathrm{int}(\tilde{\theta}) - 5 \ , \\ h^{11}(\Delta) &= \mathrm{pts}(\nabla) - \sum_{\tilde{\theta}\in\nabla_3} \mathrm{int}(\tilde{\theta}) + \sum_{\tilde{\theta}\in\nabla_2} \mathrm{int}(\tilde{\theta})\,\mathrm{int}(\theta) - 5 \ . \end{aligned} \tag{3.8}$$

The degrees of freedom to redefine the coordinates of the embedding space is accounted for by the points interior to codimension-one faces of the polyhedra. This accounts for the fact that these points do not contribute to the Hodge numbers. The terms

$$\sum_{\theta\in\Delta_2} \mathrm{int}(\theta)\,\mathrm{int}(\tilde{\theta}) \quad \text{and} \quad \sum_{\tilde{\theta}\in\nabla_2} \mathrm{int}(\tilde{\theta})\,\mathrm{int}(\theta)$$

account for non-toric deformations of the manifold.

We present in the Appendix the figures for each of the bottoms of Tables 3.2 and 3.3. In the electronic version of this article the figures are in colour and the integral points of the polyhedron are coloured according to how they contribute to Batyrev's formulas (3.8). The Dynkin diagrams are formed by the red points and lines. The points are coloured according to the following rules:

–*Black points:* These are the points that are interior to codimension one faces of the 4D polyhedron and which are subtracted in Batyrev's formulas owing to the fact that they correspond to the freedom to redefine the homogeneous coordinates of the embedding space.

–*Green points:* These are four of the five points that are subtracted off in Batyrev's formulas. They consist of the three vertices of the triangle corresponding to the torus and the first point connected to the point $(0,0,2,3)$ by an edge. The fifth point is the first point connected to the point $(0,0,2,3)$ by an edge in the top. When the polyhedron contains the point pt'_1 and its reflection in the triangle these are the points of the $K3$ polyhedron corresponding to the trivial group.

–*Blue points:* These occur only ocaisionally as in the E_8 or $SO(13)$ polyhedra. These are the points that lie interior to codimension one faces of the $K3$ polyhedron but are non-trivial owing to the fact that they *do not* lie in codimension one faces of the 4D polyhedron. These points contribute to the number of tensor multiplets. Finally we are left with the points that contribute to the rank of the group

–*Red points:* These give the Dynkin diagram of the group and, on including the first point that is connected to the point $(0, 0, 2, 3)$ by an edge we see also the extended diagram of the group with the green point as the extending point.

Of course we do not see the multiple lines of the Dynkin diagrams in the edges of the polyhedron so what we see is the 'skeleton' of the diagrams with all lines given as single lines and no distinction made between long and short roots. This being so it is fortunate that we see both the Dynkin diagram and the extended diagram in each bottom since, apart from $SO(5)$ and G_2 for which the skeletons of the diagrams are the same, these serve to uniquely identify the groups. For the cases of $SO(5)$ and G_2 the groups are distinguished on the basis of the hodge numbers.

For the bottoms of 3.3 the result of omitting the point pt'_1 is that now some of the points interior to the edges of the triangle of the torus now contribute to the rank of the group since they are no longer interior to codimension-one faces of the 4D-polyhedron.

Figures 3.3 and 3.4 show the nesting of the bottoms with the arrows denoting inclusion. Not all inclusions are shown; there are for example a number of connections between the two diagrams. It is gratifying that the majority of cases are understood as the straightforward inclusion of groups. Other cases such as $E_{6b} \to SU_{6c} \to SU_{6b}$ would seem to indicate the possibility of non-perturbative transitions.

Finally we return to discuss the structure of the tops. As given in Table 3.5, these do not as pleasing an interpretation as the bottoms. In particular not all of the points of the Dynkin diagrams are visible. For example the top for $k = 3/2$ corresponds to the group $G_2^{(0)} = SU(3)$ but is the reflection, in the triangle of the torus, of the $SU(2)$ bottom. Additionally the $k = 5/2$ and $k = 3$ tops are the same, being the reflection of the F_4 bottom, though the corresponding groups are $G_2^{(0)} = F_4$ and $G_2^{(0)} = E_6$. This suggests that the 'missing' points should be added to the tops. This can be done by replacing the tops by the reflections of the bottoms for the groups $G_2^{(0)}$ except that $SO(9)$ should be used instead of $SO(8)$ and E_7 in place of what we have called E_7^-. The Hodge numbers are unchanged by this process. The reason that the points that contribute to the rank of the group were not previously visible is that although the previously given tops give the correct values for the Hodge numbers they correspond, for those cases for which the Dynkin diagram is not fully visible, to manifolds with non-toric parameters *i.e.,* to polyhedra for which the correction term in Batyrev's formulas is non-zero. By adding the extra points to the tops the correction term disappears so that now all the parameters are torically expressed.

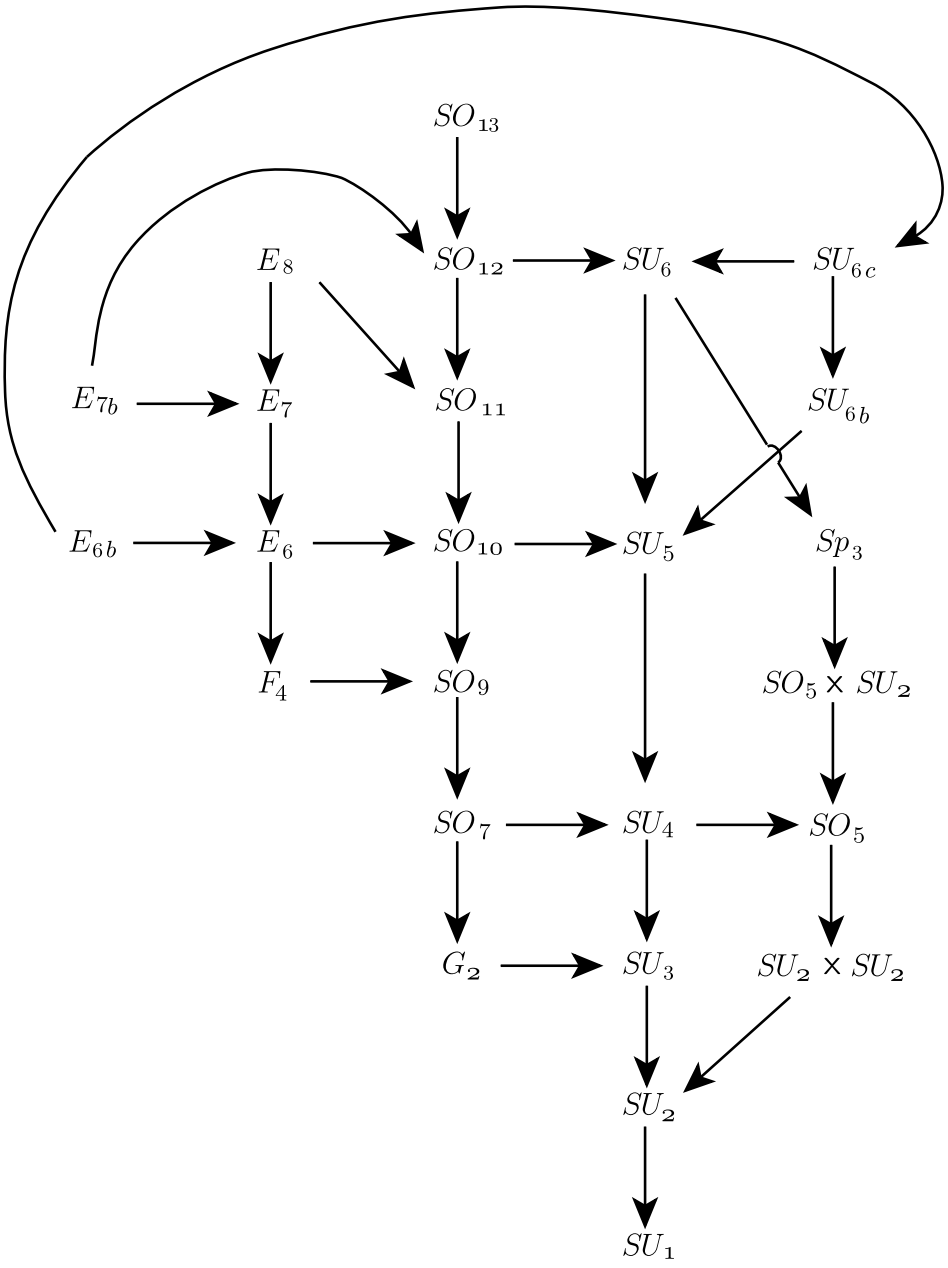

Figure 3.3: Inclusion of polyhedra for the polyhedra that contain the point pt'_1. The arrows denote inclusion of the bottoms.

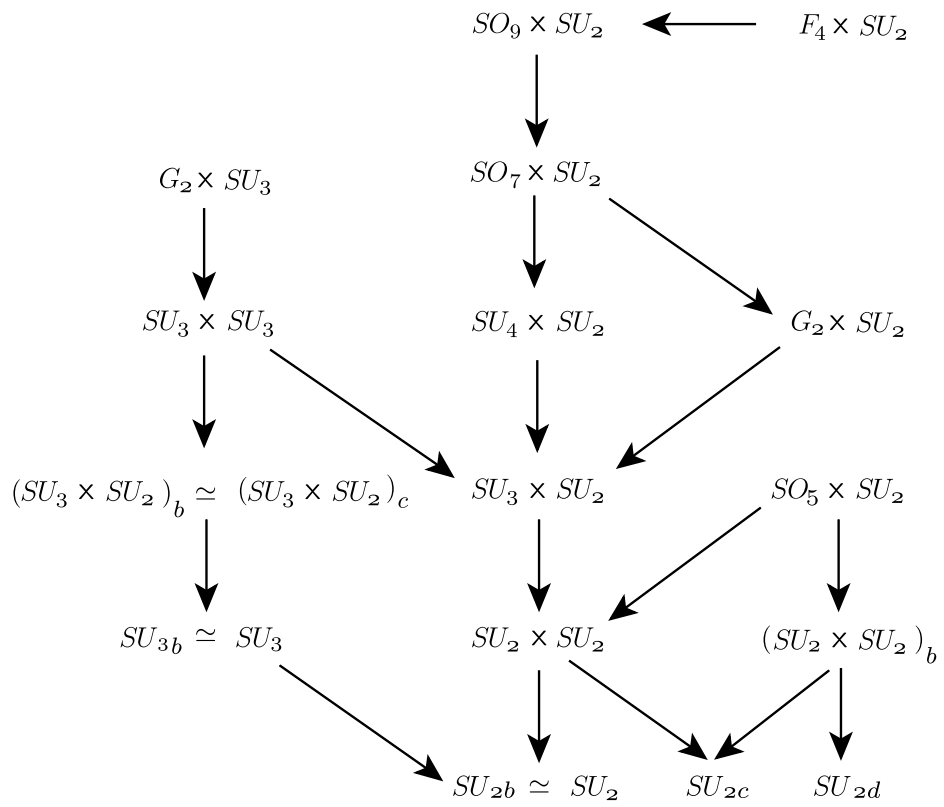

Figure 3.4: Inclusion of polyhedra for the polyhedra that do not contain the point pt'_1. This figure has been drawn on the assumption that some of the polyhedra correspond to the same Calabi–Yau manifold. This hypothesized equivalence is denoted by $\sim$ in the diagram.

4. **Discussion**

In this article we have considered $K3 \times T^2$, $E_8 \times E_8$ compactifications with instanton numbers (d_1, d_2) and n_T tensor multiplets. Matching of spectra [1,8], and arguments based on F-theory [36,35], indicate that at the points of maximal symmetry breaking heterotic theories of this type are dual to type IIA compactifications on Calabi–Yau manifolds that admit a $K3$ as well as an elliptic fibration. The new contribution here is the observation that sequences of reflexive polyhedra associated to these spaces are nested in such a way as to reflect heterotic perturbative and non-perturbative processes. This qualitative observation is supported by quantitative agreement of the computed Hodge numbers and the number of tensor, vector and hypermultiplets in the heterotic side. It leads also to the observation that the Dynkin diagrams for the groups may be read off from the polyhedra.

The results displayed in Tables 3.2 and 3.3 correspond to reflexive polyhedra that can be formed by adding the points $pt_r^{(j)}$ to $\nabla_{\rm bot}^{SU(1)}$. It is also possible to extend the bottoms by adding points that are not directly below the pt_r. It is clear that there are other groups that can be realised in this way but a systematic investigation will require an efficient way of enumerating possibilities. Also of considerable interest is the issue of which points may be added in the fourth dimension. These four dimensional points are very interesting since they are associated with non-perturbative effects. We have touched on some of these issues with the polyhedra $\nabla^{H,k,j}$ but this is clearly just scratching the surface of possibilities.

In the heterotic picture, $E_8 \times E_8$ is broken to a generic $G_1 \times G_2$ group by background fields with (d_1, d_2) instanton numbers. In terms of polyhedra we have only found the equivalent description of processes in which G_2 remains maximally broken while A, D, and E group factors in G_1 are perturbatively restored. In the non-perturbative effects that were observed, G_2 also remains stable. Since we have not seen signals of G_2 dynamics, expected at least for some d_2, we presume that they will arise upon more generic manipulations of the polyhedra.

In summary, we have uncovered the beginnings of a dictionary that translates between vector bundles and polyhedra. The precise nature of this dictionary remains for future work.

While this article was being completed we received two articles[48,49] which overlap with the present work.

Acknowledgements

We had the benefit of useful conversations with G. Aldazabal, P. Aspinwall, X. de la Ossa, L. Ibáñez, V. Kaplunovsky, S. Katz, F. Quevedo and A. Uranga. This work was supported in part by the Robert A. Welch Foundation and the NSF grant PHY-9511632. A.F. acknowledges a research grant Conicit-S1-2700 and a CDCH-UCV sabbatical fellowship.

A. **Appendix: Tables of Hodge Numbers and Figures**

Tables of Hodge numbers calculated from the polyhedra are shown on the following pages together with plots of a selection of tops and bottoms of the polyhedra.

k	$SU(1)$	$SU(2)$	$SU(3)$	$SU(4)$	$SU(5)$	$SO(10)$	E_6	E_7
0	(243, 3)	(214, 4)	(197, 5)	(182, 6)	(167, 7)	(164, 8)	(159, 9)	(152, 10)
$\frac{1}{2}$	(243, 3)	(202, 4)	(179, 5)	(160, 6)	(142, 7)	(138, 8)	(132, 9)	(124, 10)
1	(243, 3)	(190, 4)	(161, 5)	(138, 6)	(117, 7)	(112, 8)	(105, 9)	(96, 10)
$\frac{3}{2}$	(251, 5)	(186, 6)	(151, 7)	(124, 8)	(100, 9)	(94, 10)	(86, 11)	(76, 12)
2	(271, 7)	(194, 8)	(153, 9)	(122, 10)	(95, 11)	(88, 12)	(79, 13)	(68, 14)
$\frac{5}{2}$	(295, 7)	(206, 8)	(159, 9)	(124, 10)	(94, 11)	(86, 12)	(76, 13)	(64, 14)
3	(321, 9)	(220, 10)	(167, 11)	(128, 12)	(95, 13)	(86, 14)	(75, 15)	(62, 16)
$\frac{7}{2}$	(348, 10)	(235, 11)	(176, 12)	(133, 13)	(97, 14)	(87, 15)	(75, 16)	(61, 17)
4	(376, 10)	(251, 11)	(186, 12)	(139, 13)	(100, 14)	(89, 15)	(76, 16)	(61, 17)
$\frac{9}{2}$	(404, 14)	(267, 15)	(196, 16)	(145, 17)	(103, 18)	(91, 19)	(77, 20)	(61, 21)
5	(433, 13)	(284, 14)	(207, 15)	(152, 16)	(107, 17)	(94, 18)	(79, 19)	(62, 20)
$\frac{11}{2}$	(462, 12)	(301, 13)	(218, 14)	(159, 15)	(111, 16)	(97, 17)	(81, 18)	(63, 19)
6	(491, 11)	(318, 12)	(229, 13)	(166, 14)	(115, 15)	(100, 16)	(83, 17)	(64, 18)

Table A.1: The Hodge numbers (h^{21}, h^{11}) calculated from the polyhedra $\nabla^{k,H}$ for the chain $H = SU(1), \ldots, SU(5)$, $SO(10)$, E_6, E_7.

k	$SU(2)^2$	$SU(2)^3$	$SO(8)$	$SU(6)$	$SU(6)_b$	$SO(12)$
0	(185, 5)	(156, 6)	(175, 7)	(152, 8)	(150, 8)	(149, 9)
$\frac{1}{2}$	(165, 5)	(132, 6)	(151, 7)	(125, 8)	(122, 8)	(121, 9)
1	(145, 5)	(108, 6)	(127, 7)	(98, 8)	(94, 8)	(93, 9)
$\frac{3}{2}$	(133, 7)	(92, 8)	(111, 9)	(79, 10)	(74, 10)	(73, 11)
2	(133, 9)	(88, 10)	(107, 11)	(72, 12)	(66, 12)	(65, 13)
$\frac{5}{2}$	(137, 9)	(88, 10)	(107, 11)	(69, 12)	(62, 12)	(61, 13)
3	(143, 11)	(90, 12)	(109, 13)	(68, 14)	(60, 14)	(59, 15)
$\frac{7}{2}$	(150, 12)	(93, 13)	(112, 14)	(68, 15)	(59, 15)	(58, 16)
4	(158, 12)	(97, 13)	(116, 14)	(69, 15)	(59, 15)	(58, 16)
$\frac{9}{2}$	(166, 16)	(101, 17)	(120, 18)	(70, 19)	(59, 19)	(58, 20)
5	(175, 15)	(106, 16)	(125, 17)	(72, 18)	(60, 18)	(59, 19)
$\frac{11}{2}$	(184, 14)	(111, 15)	(130, 16)	(74, 17)	(61, 17)	(60, 18)
6	(193, 13)	(116, 14)	(135, 15)	(76, 16)	(62, 16)	(61, 17)

Table A.2: The Hodge numbers (h^{21}, h^{11}) calculated from the polyhedra $\nabla^{k,H}$ for the groups $SU(2)^2$, $SU(2)^3$, $SO(8)$, $SU(6)$, $SU(6)_b$ and $SO(12)$.

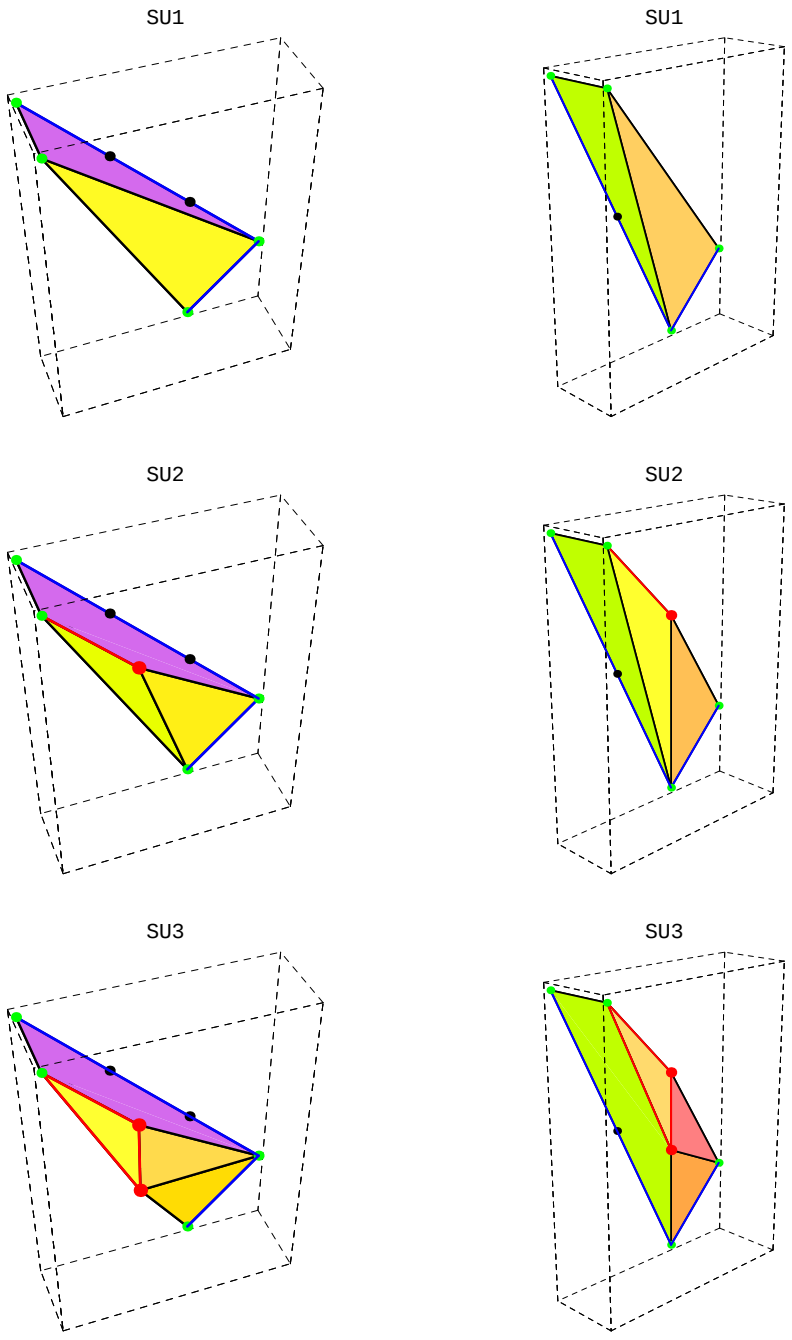

Figure A.1: Two views of the polyhedra for each of the indicated groups.

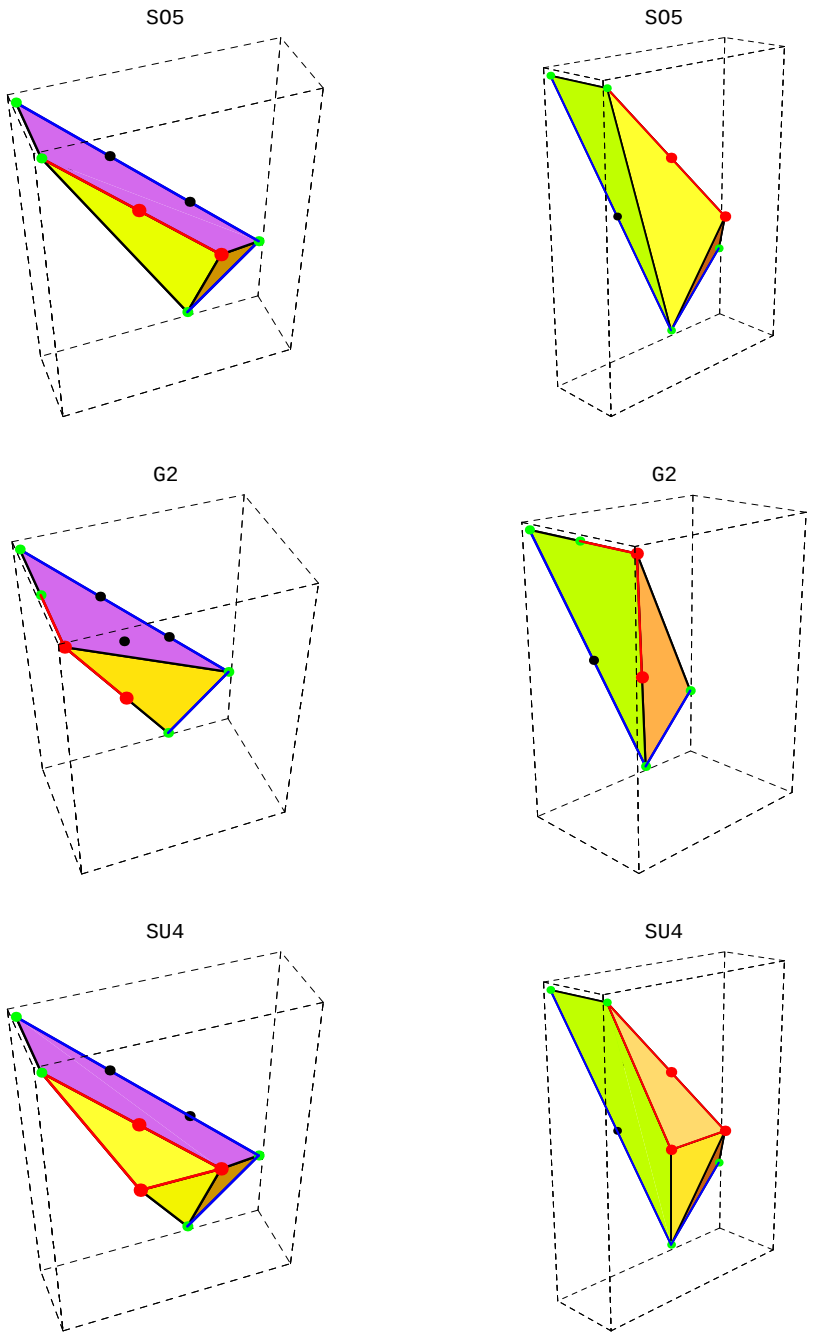

Figure A.2: Two views of the polyhedra for each of the indicated groups.

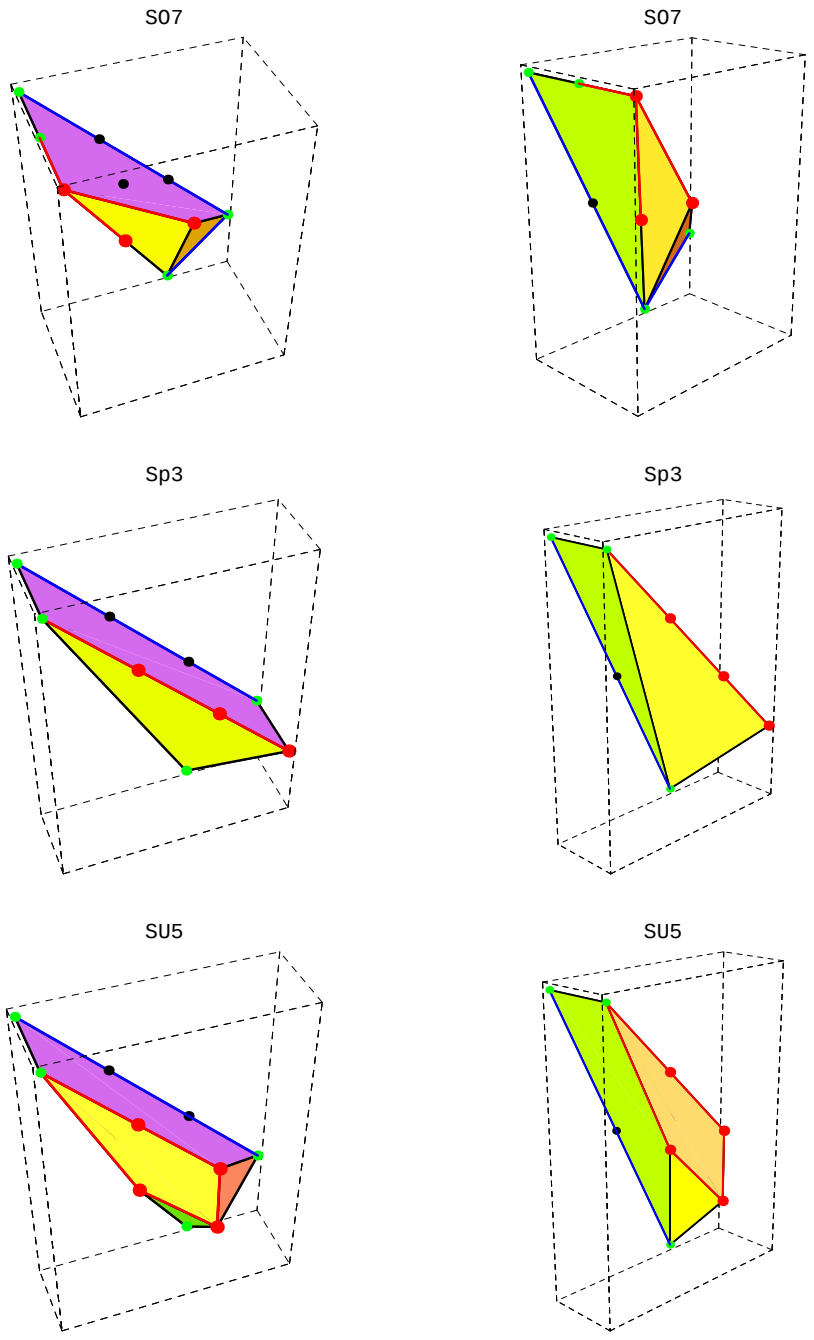

Figure A.3: Two views of the polyhedra for each of the indicated groups.

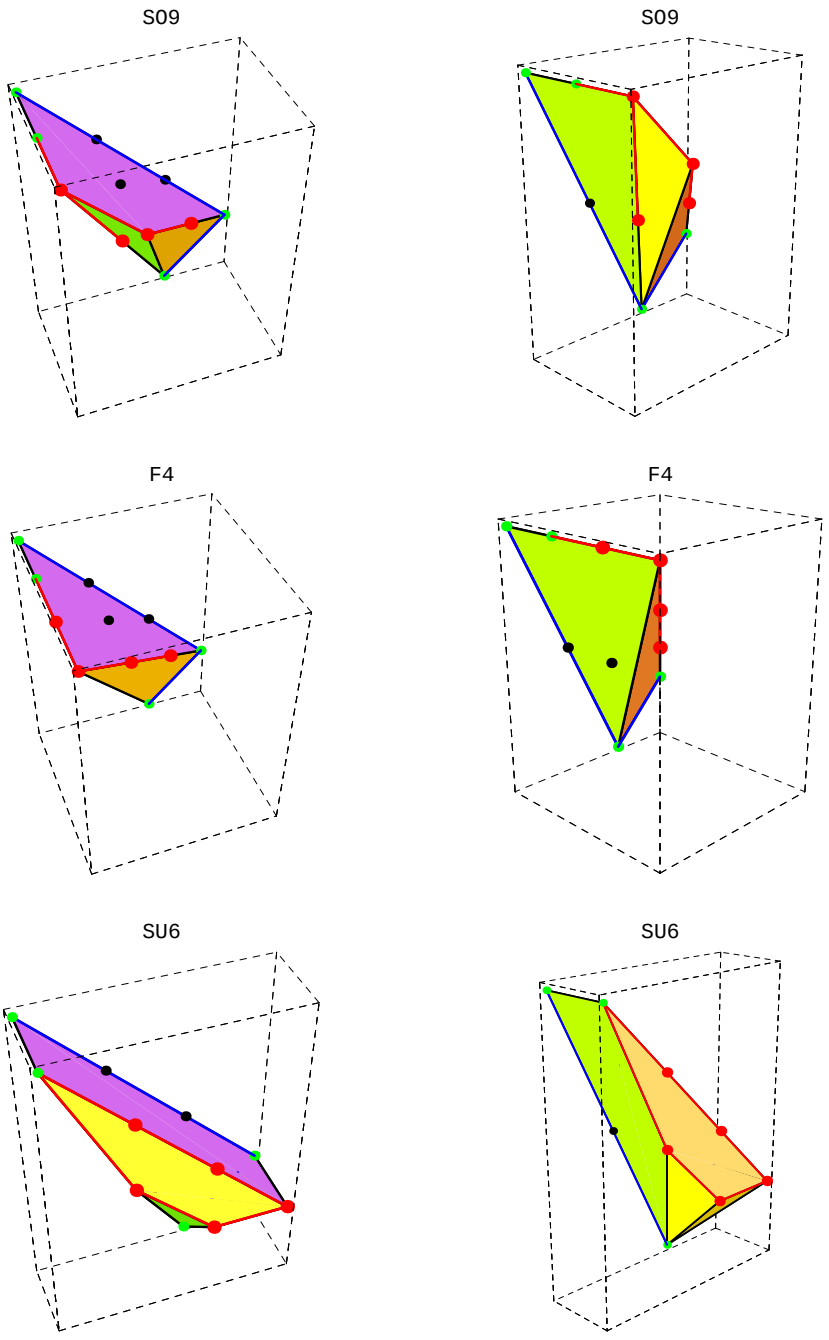

Figure A.4: Two views of the polyhedra for each of the indicated groups.

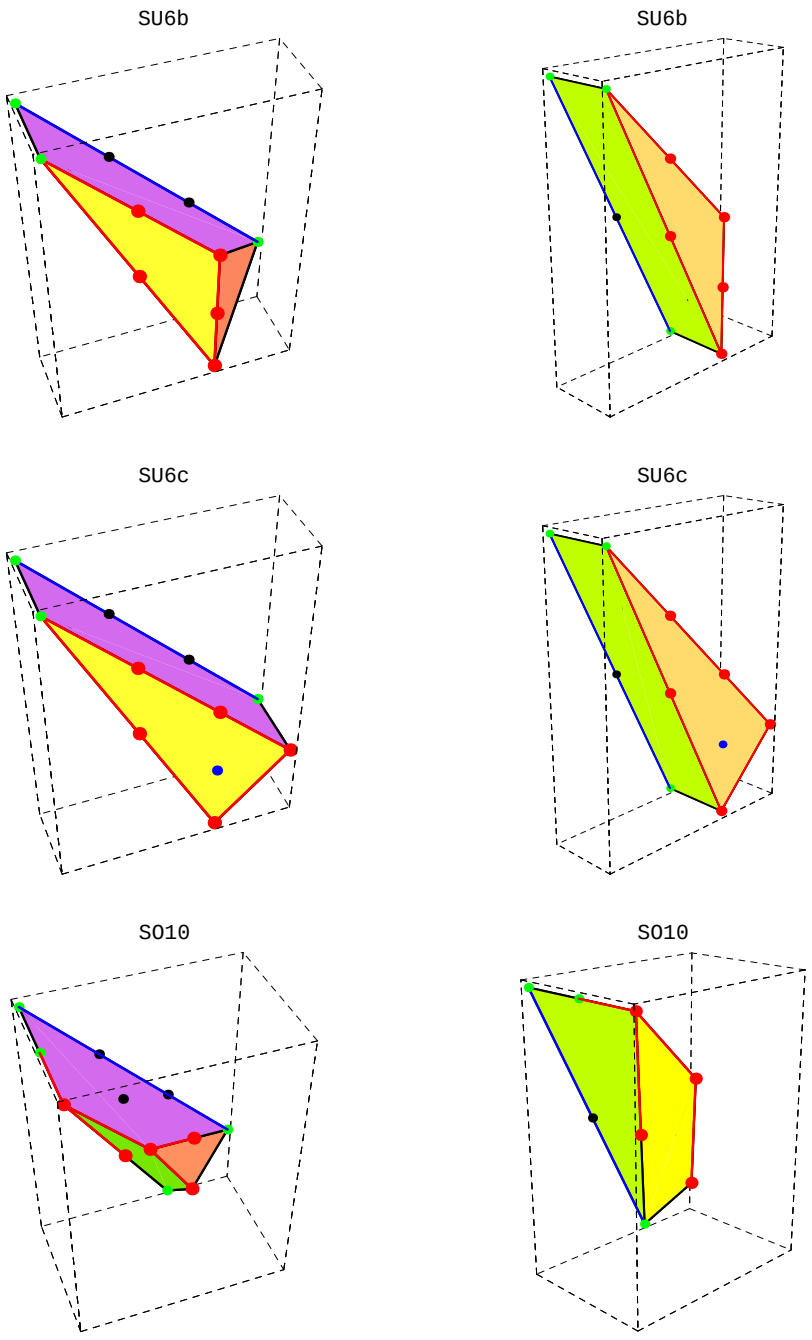

Figure A.5: Two views of the polyhedra for each of the indicated groups.

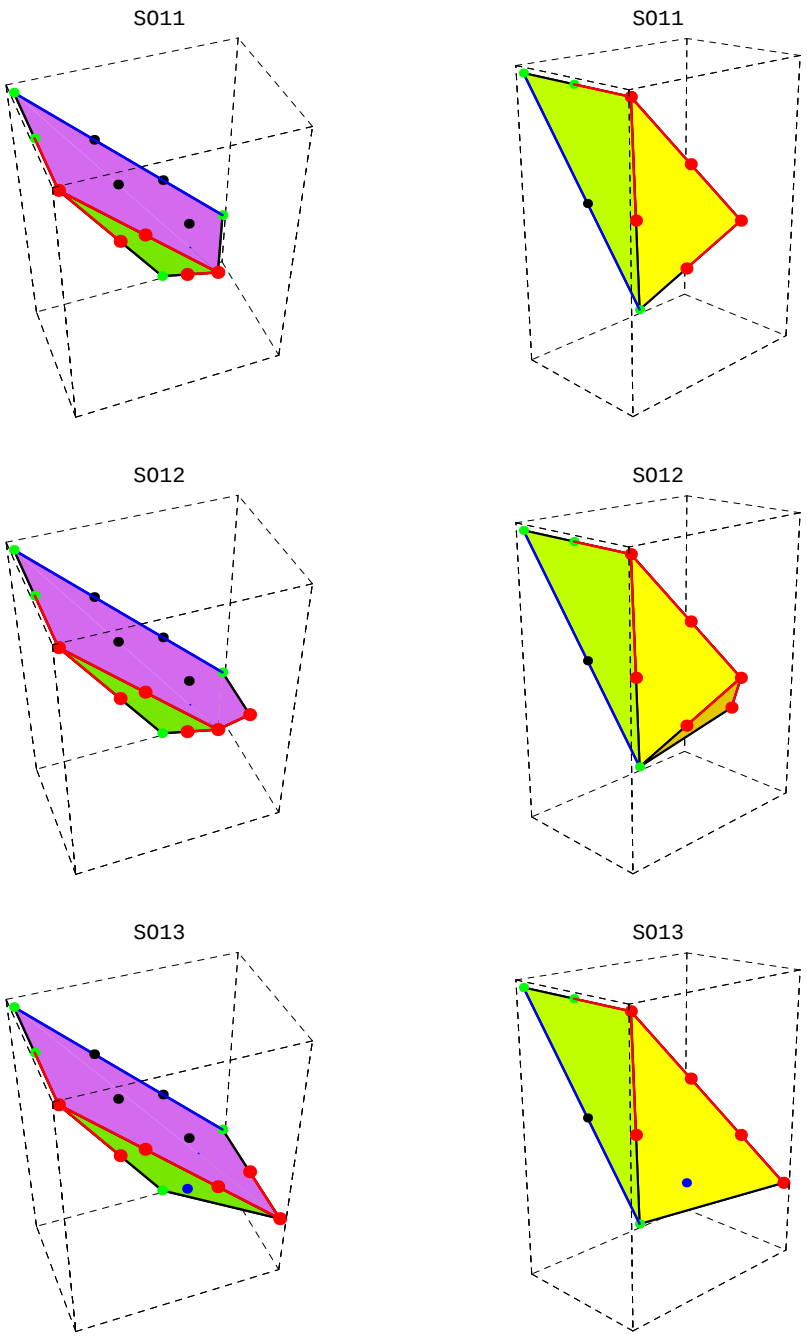

Figure A.6: Two views of the polyhedra for each of the indicated groups.

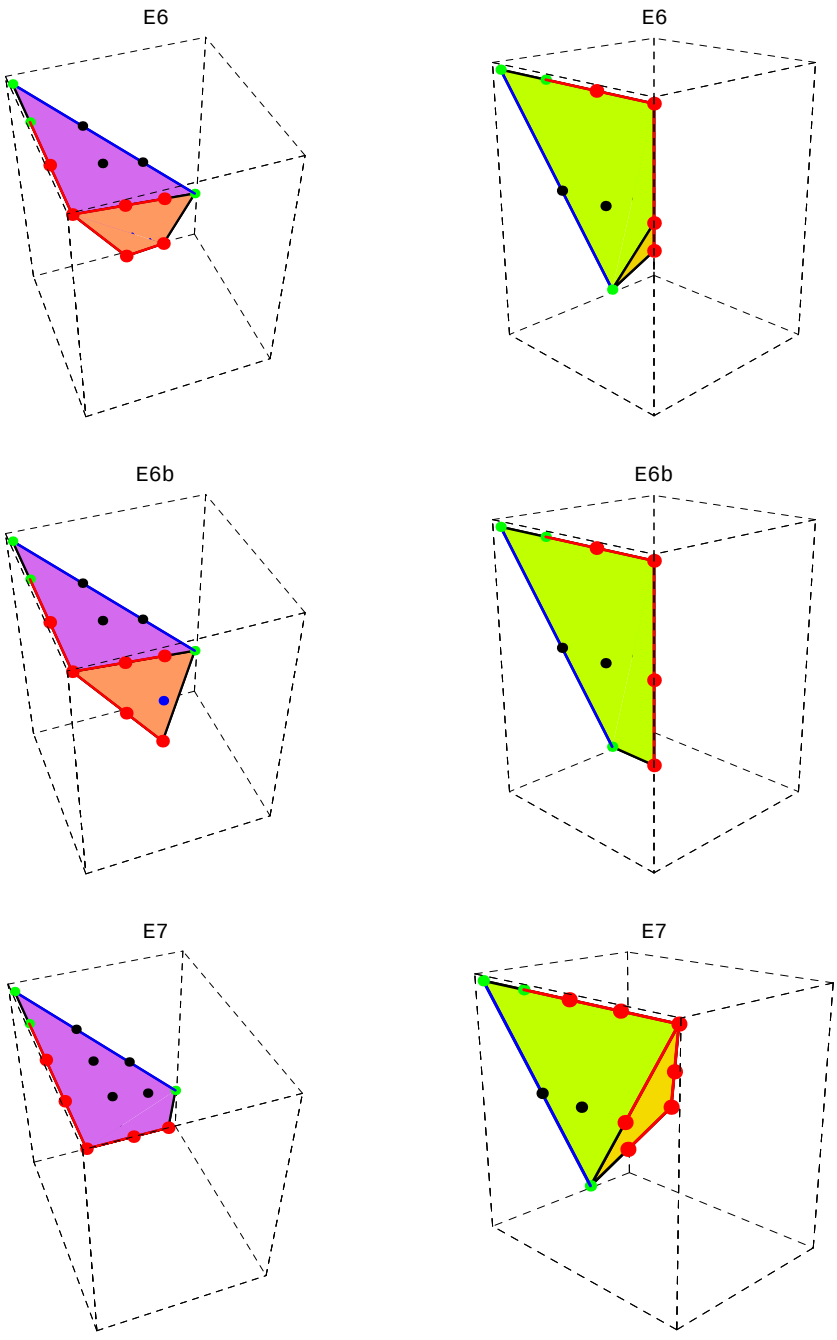

Figure A.7: Two views of the polyhedra for each of the indicated groups.

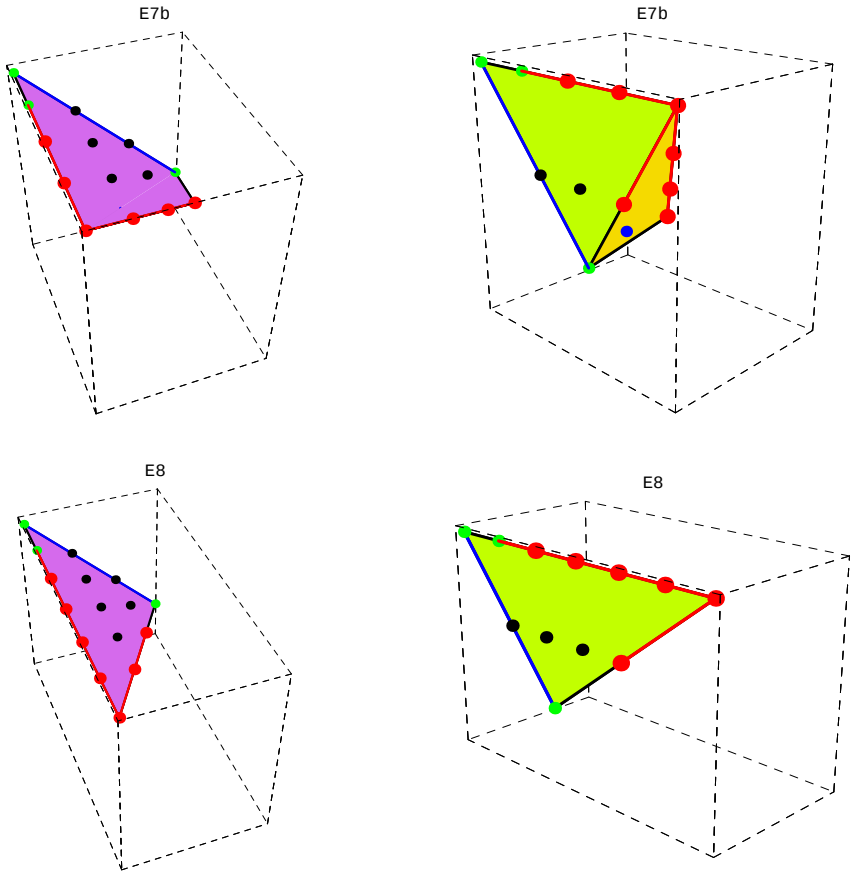

Figure A.8: Two views of the polyhedra for each of the indicated groups.

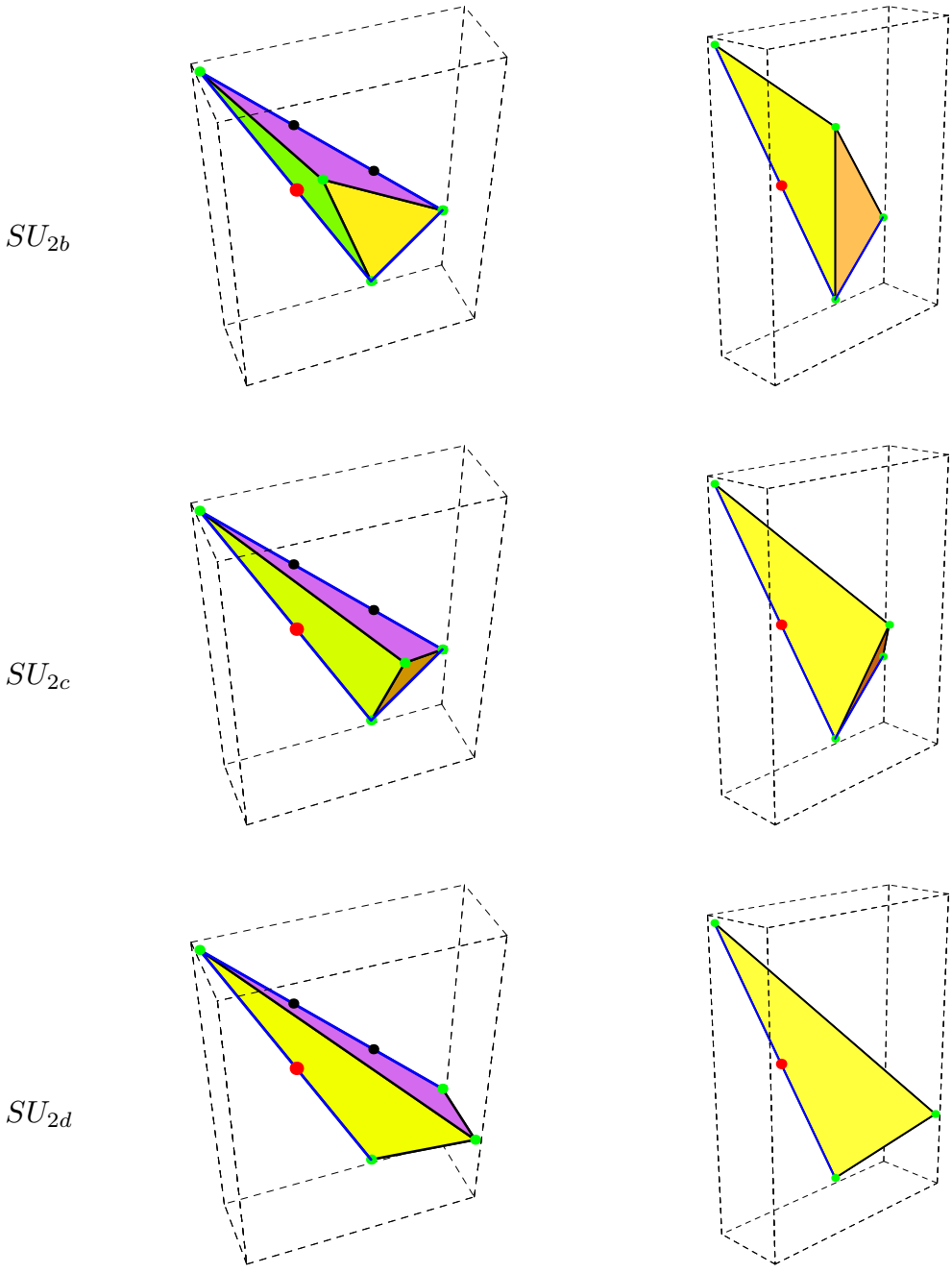

Figure A.9: Two views of the polyhedra for each of the indicated groups.

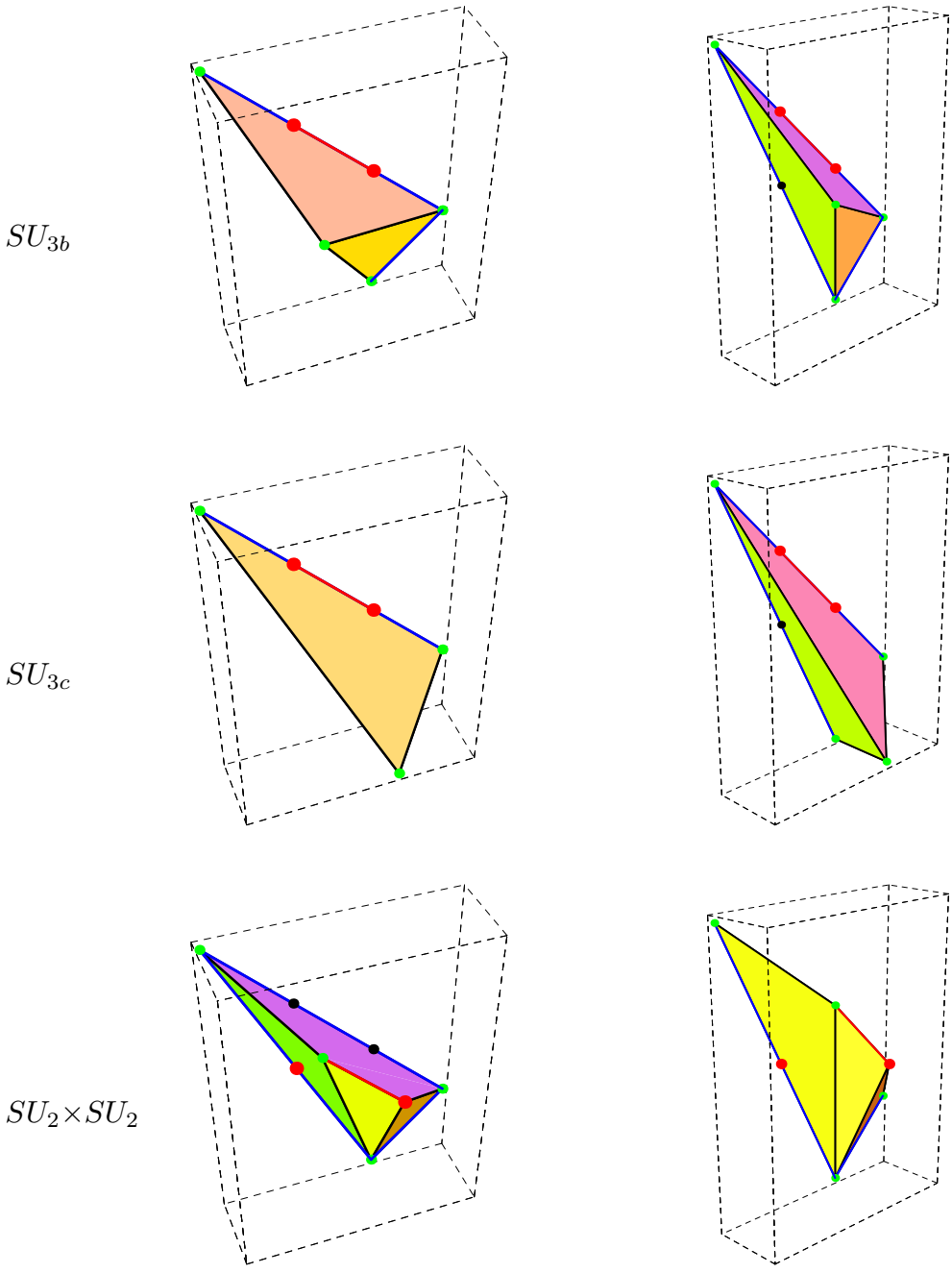

Figure A.10: Two views of the polyhedra for each of the indicated groups.

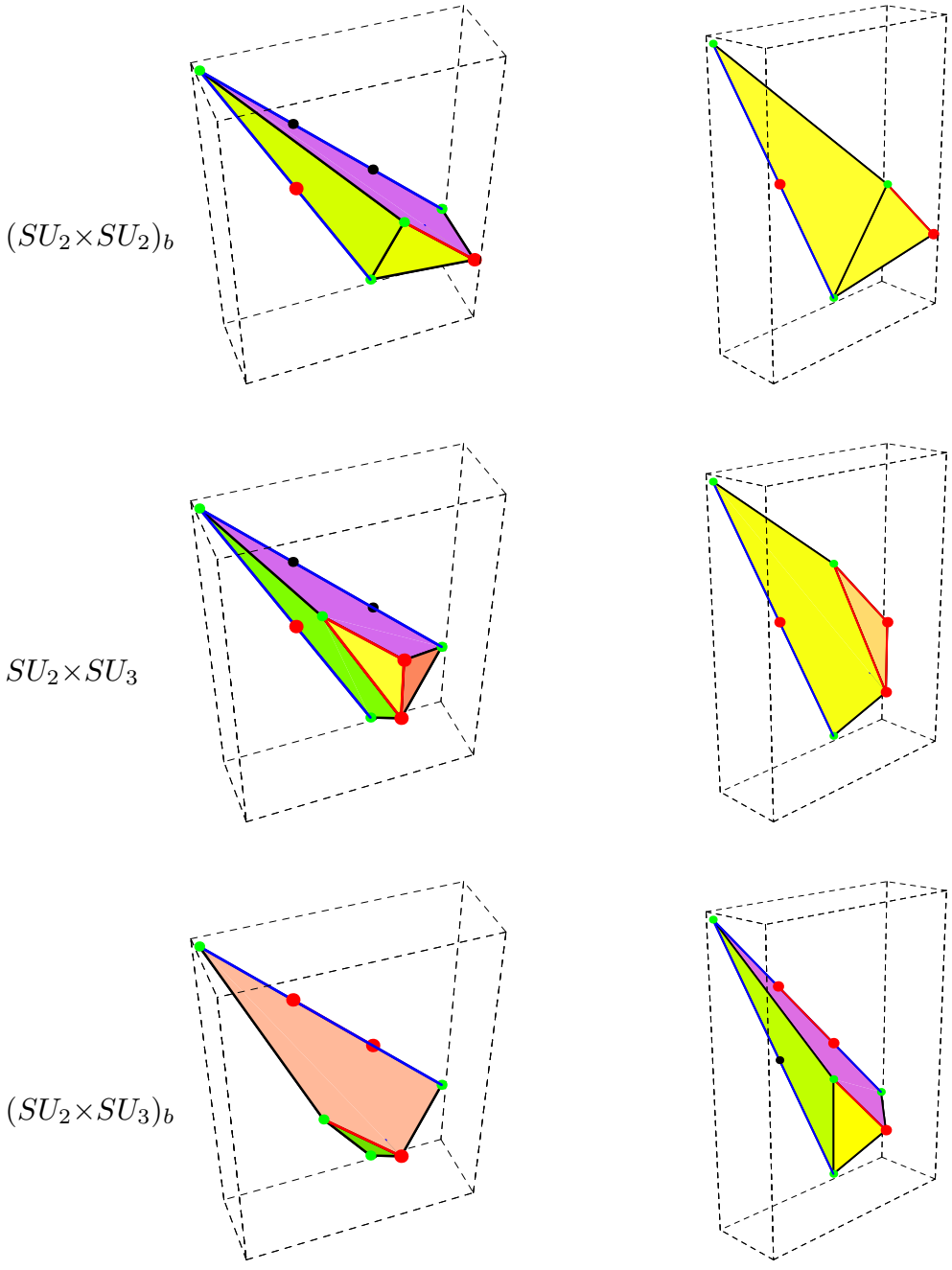

Figure A.11: Two views of the polyhedra for each of the indicated groups.

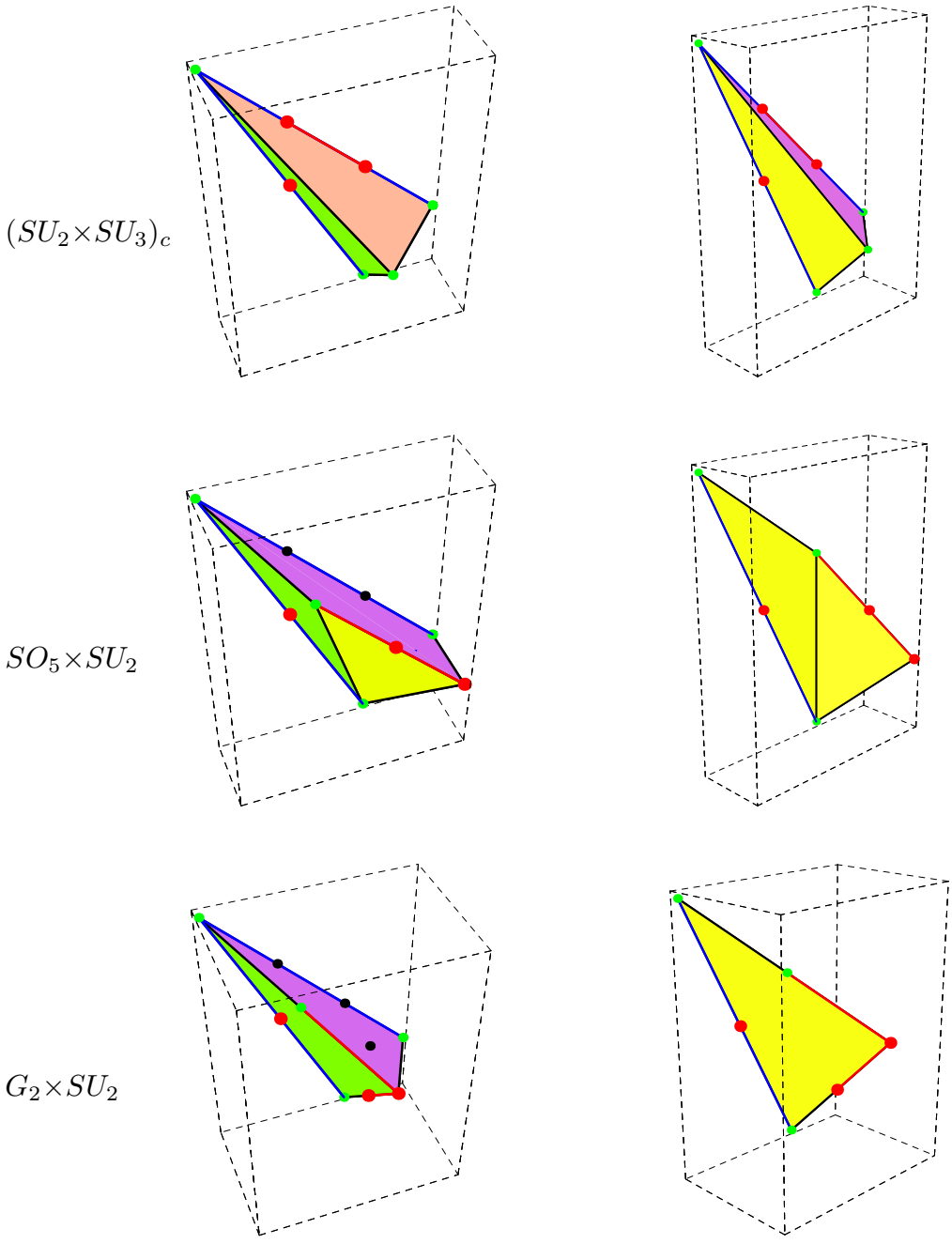

Figure A.12: Two views of the polyhedra for each of the indicated groups.

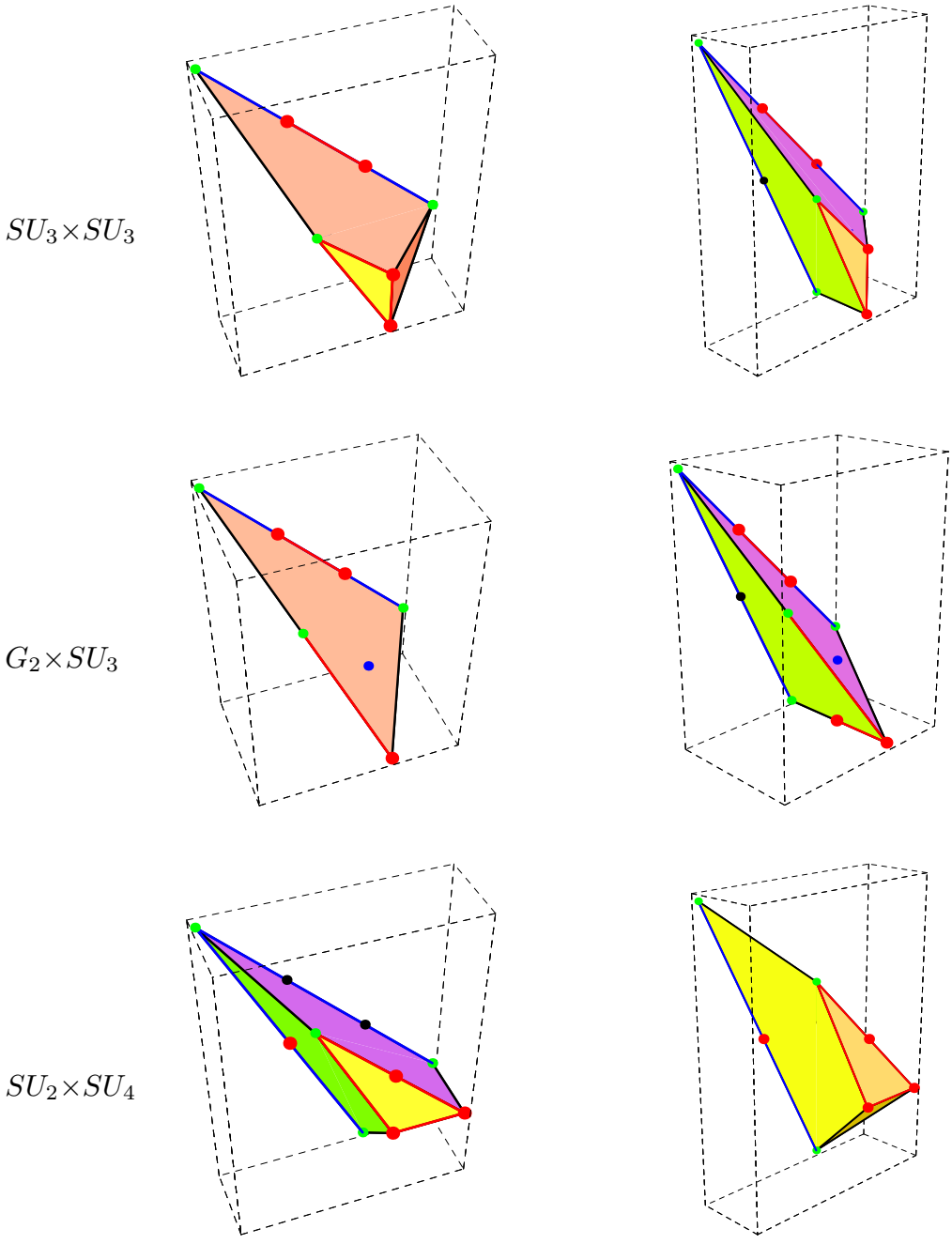

Figure A.13: Two views of the polyhedra for each of the indicated groups.

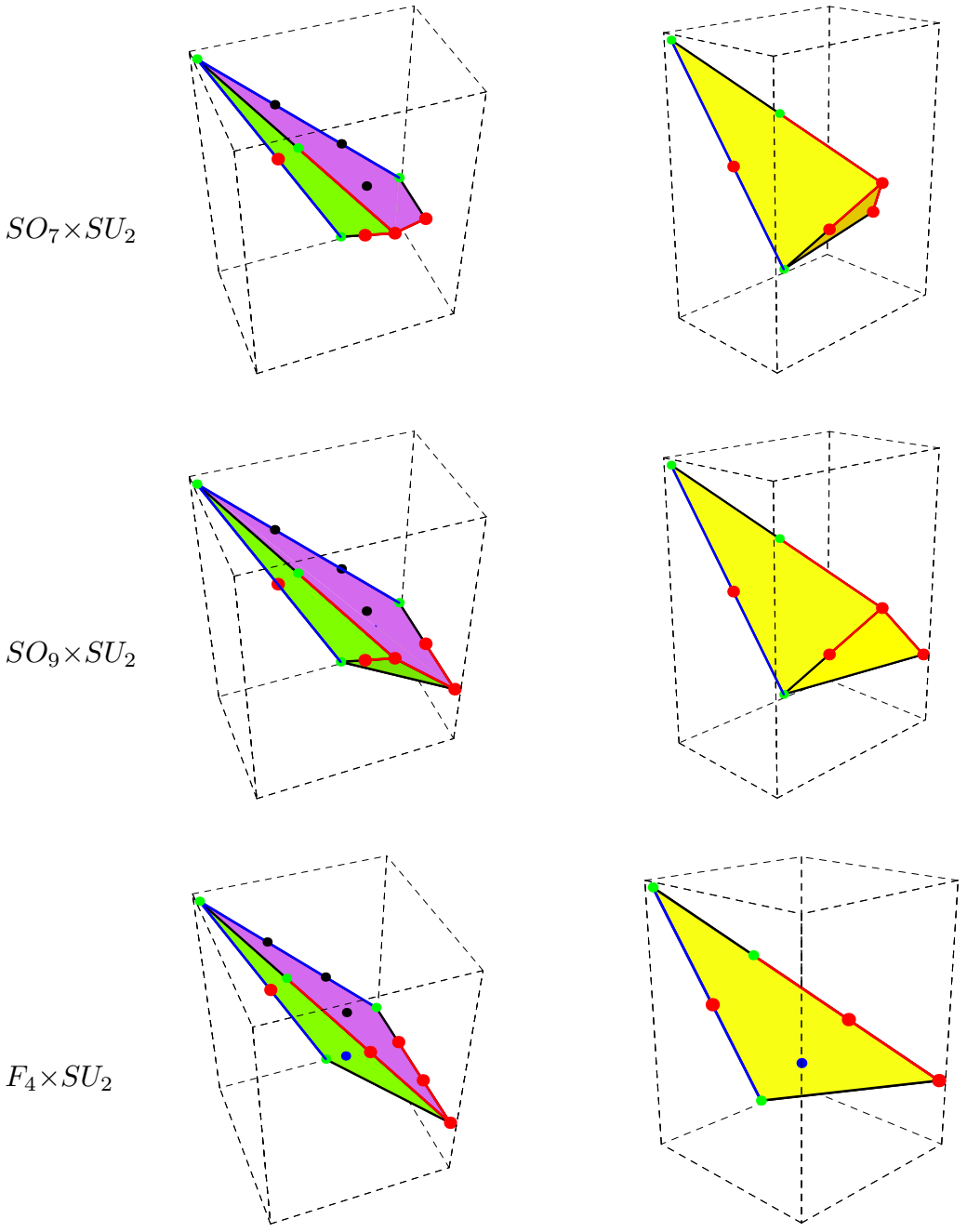

Figure A.14: Two views of the polyhedra for each of the indicated groups.

References

1. S. Kachru and C. Vafa, Nucl. Phys. **B450** (1995) 69, hep-th/9505105.
2. S. Ferrara, J. Harvey, A. Strominger and C. Vafa,
   Phys. Lett. **361B** (1995) 59, hep-th/9505162.
3. A. Klemm, W. Lerche, and P. Mayr, Phys. Lett. **357B** (1995) 313, hep-th/9506112.
4. C. Vafa and E. Witten, hep-th/9507050.
5. C. Gómez and E. López, Phys. Lett. **356B** (1995) 487, hep-th/9506024;
   M. Billó, A. Ceresole, R. D'Auria, S. Ferrara, P. Fré, T. Regge, P. Soriani and A. van Proyen, hep-th/9506075;
   I. Antoniadis, E. Gava, K.S. Narain and T.R. Taylor,
   Nucl. Phys. **B455** (1995) 109, hep-th/9507115;
   G. Lopes Cardoso, D. Lust and T. Mohaupt,
   Nucl. Phys. **B455** (1995) 131, hep-th/9507113;
   G. Curio, Phys. Lett. **368B** (1996) 78, hep-th/9509146.
6. V. Kaplunovsky, J. Louis and S. Theisen,
   Phys. Lett. **357B** (1995) 71, hep-th/9506110.
7. S. Kachru, A. Klemm, W. Lerche, P. Mayr and C. Vafa,
   Nucl. Phys. **B459** (1996) 537, hep-th/9508155.
8. G. Aldazabal, A. Font, L. E. Ibáñez and F. Quevedo,
   Nucl. Phys. **B461** (1996) 85, hep-th/9510093.
9. P. S. Aspinwall and J. Louis, Phys. Lett. **369B** (1996) 233, hep-th/9510234.
10. P. S. Aspinwall, Phys. Lett. **371B** (1996) 231, hep-th/9511171.
11. B. Hunt and R. Schimmrigk, hep-th/9512138;
    R. Blumenhagen and A. Wisskirchen, hep-th/9601050.
12. A. Klemm and P. Mayr hep-th/9601014.
13. P. Berglund, S. Katz and A. Klemm, in preparation.
14. A. Klemm and R. Schimmrigk, Nucl. Phys. **B411** (1994) 559, hep-th/9204060.
15. M. Kreuzer and H. Skarke, Nucl. Phys. **B388** (1992) 113, hep-th/9205004.
16. P. Candelas, X. de la Ossa and S. Katz,
    Nucl. Phys. **B450** (1995) 267, hep-th/9412117.
17. H. Skarke, alg-geom/9603007.
18. V. Batyrev, Duke Math. Journ. **69** (1993) 349.
19. M. Reid, Math. Ann. **278** (1987) 329.
20. P. Candelas, A.M. Dale, C.A. Lütken, R. Schimmrigk,
    Nucl. Phys. **B298** (1988) 493.

21. P. Candelas, P.S. Green and T. Hübsch, Nucl. Phys. **B330** (1990) 49.

22. P. S. Aspinwall, B.R. Greene and D.R. Morrison,
Int. Math. Res. Notices (1993) 319, alg-geom/9309007.

23. P. Berglund, S. Katz and A. Klemm, Nucl. Phys. **B456** (1995) 153, hep-th/9506091.

24. M. Lynker and R. Schimmrigk, hep-th/9511058.

25. A. C. Avram, P. Candelas, D. Jančić and M. Mandelberg, hep-th/9511230.

26. T.-M. Chiang, B. R. Greene, M. Gross and Y. Kanter, hep-th/9511204.

27. A. Strominger, Nucl. Phys. **B451** (1995) 96, hep-th/9504090.

28. B. Greene, D. R. Morrison and A. Strominger,
Nucl. Phys. **B451** (1995) 109, hep-th/9504145.

29. M. Bershadsky, V. Sadov and C. Vafa, hep-th/9510225.

30. S. Katz, D. R. Morrison and M. R. Plesser, hep-th/9601108.

31. E. Witten, Nucl. Phys. **B460** (1996) 541, hep-th/9511030.

32. M. Duff, R. Minasian and E. Witten, hep-th/9601036.

33. N. Seiberg and E. Witten, hep-th/9603003.

34. A. Uranga, unpublished.

35. D. Morrison and C. Vafa, hep-th/9602114.

36. C. Vafa, hep-th/9602022.

37. G. Aldazabal, A. Font, L. E. Ibáñez and F. Quevedo, hep-th/9602097.

38. P. S. Aspinwall and M. Gross, hep-th/9602118.

39. J. Erler, J. Math. Phys. 35 (1993) 377, hep-th/9304104.

40. P. Horava and E. Witten, Nucl. Phys. **B460** (1996) 506, hep-th/9510209.

41. E. Witten, hep-th/9512219.

42. V. Kaplunovsky, private communication.

43. A. Uranga, private communication.

44. G. Aldazabal, L. E. Ibáñez and A. Uranga, unpublished.

45. M. Bershadsky, K. Intriligator, S. Kachru, D. R. Morrison, V. Sadov and C. Vafa,
Nucl. Phys. **B481** (1996) 215, hep-th/9605200.

46. V. Batyrev, J. Alg. Geom. **3** (1994) 493, alg-geom/9310003.

47. P. S. Aspinwall, B. R. Greene and D. R. Morrison, Int. Math. Res. Notices (1993)
319, alg-geom/9309007.

48. E. Witten, hep-th/9603150.

49. D. R. Morrison and C. Vafa, hep-th/9603161.